Constraining Fundamental Physics with current Cosmological Data

24th November 2014, Hamburg

Eleonora Di Valentino
Institut d’Astrophysique de Paris

Outline:

- The CMB
- The neutrino effective number N_{eff}
- The sum of active neutrino masses
- The sterile neutrino mass
- Axion cosmology
- Neutrino isocurvature density
- The rate A_2 of the radiative capture reaction $d(p;\gamma)^3He$
- Conclusions

The CMB

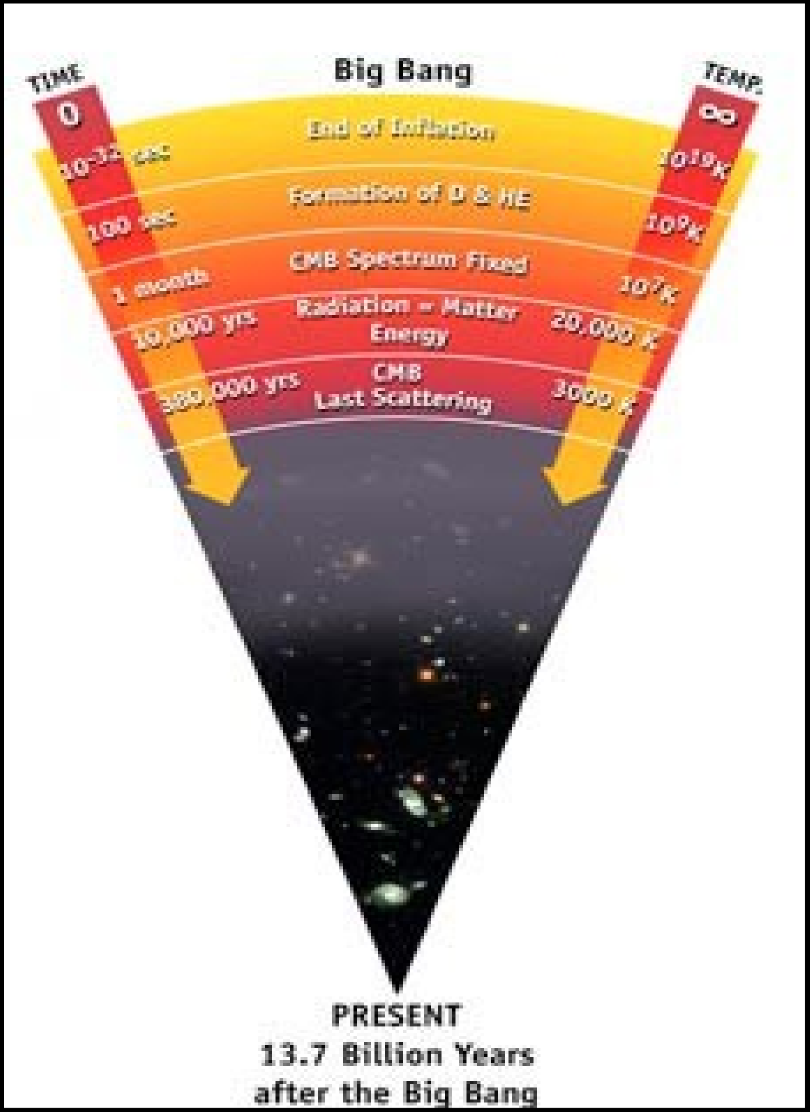

The Universe originates from a hot Big Bang. The primordial plasma in thermodynamic equilibrium cools with the expansion of the Universe. It passes through the phase of recombination, where electrons and protons combine into hydrogen atoms, and the phase of decoupling, in which the Universe becomes trasparent to the motion of photons.

The Cosmic Microwave Background (CMB) is the radiation emitted about 13 billion years ago, just 400,000 years after the Big Bang. The CMB provides an unexcelled probe of the early Universe and today it is a black body a temperature T=2.7255K.

The CMB

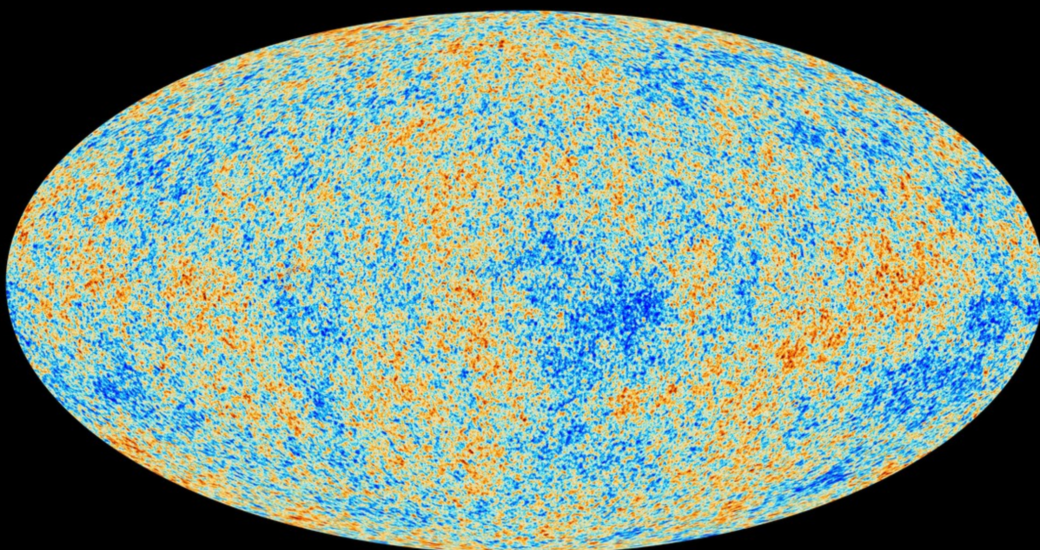

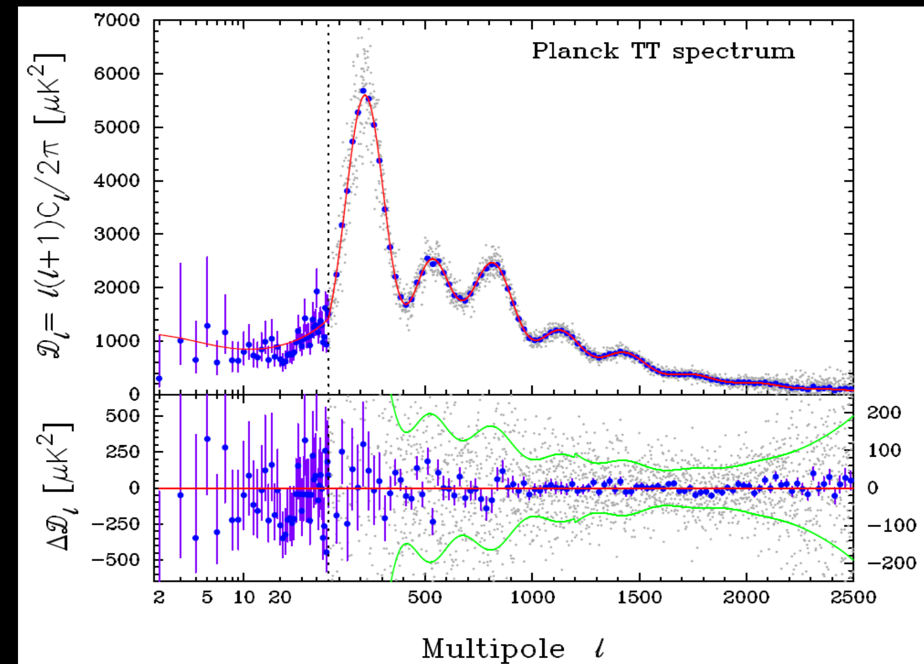

Ade et al., arXiv:1303.5076

The main tool of research in cosmology is the angular power spectrum of CMB temperature anisotropies.

$$\left\langle \frac{\Delta T}{T}(\vec{\gamma}_1)\frac{\Delta T}{T}(\vec{\gamma}_2)\right\rangle = \frac{1}{2\pi}\sum_{\ell}(2\ell+1)C_\ell P_\ell(\vec{\gamma}_1\cdot\vec{\gamma}_2)$$

The CMB

Cosmological parameters:
($\Omega_b h^2$, $\Omega_m h^2$, h , n_s , τ, Σm_ν)

Theoretical model

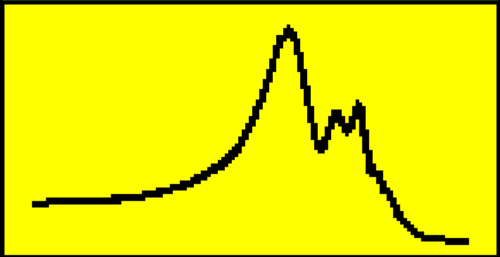

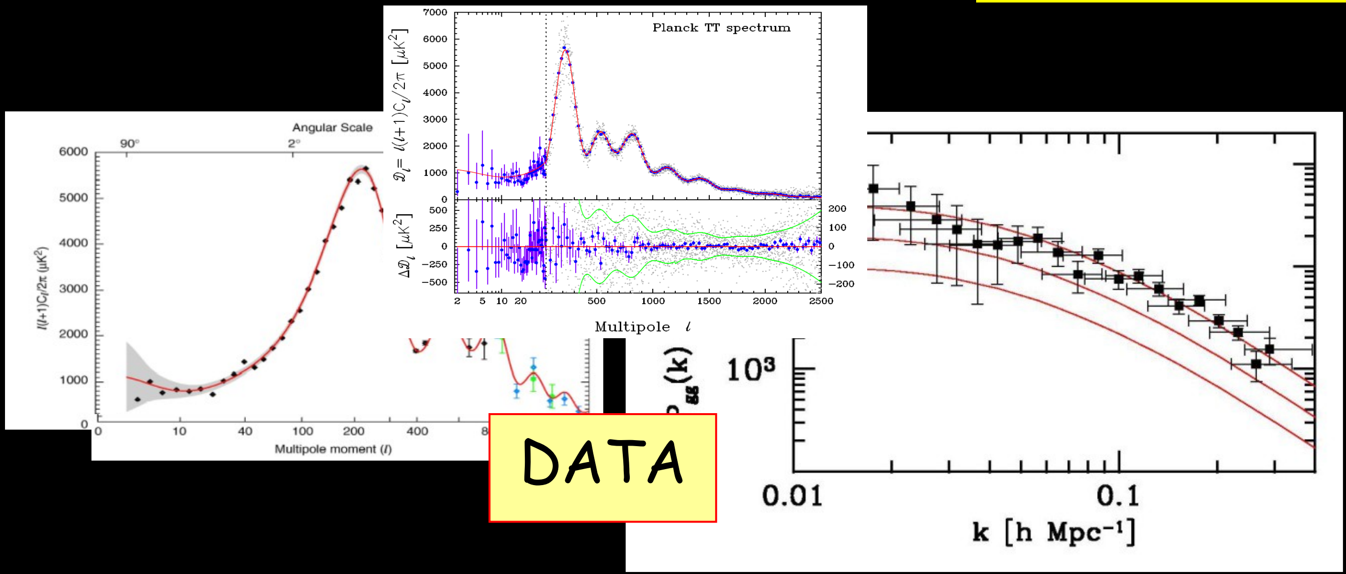

PARAMETER CONSTRAINTS

The Cosmic Neutrino Background

When the rate of the weak interaction reactions, which keep neutrinos in equilibrium with the primordial plasma, becomes smaller than the expansion rate of the Universe, neutrinos decouple at a temperature of about:

$$T_{dec} \approx 1 MeV$$

After neutrinos decoupling, photons are heated by electrons-positrons annihilation. When also photons decouple, the ratio between the temperatures of photons and neutrinos will be fixed, despite the temperature decreases with the expansion of the Universe. We expect today a Cosmic Neutrino Background (CNB) at a temperature:

$$T_\nu = \left(\frac{4}{11}\right)^{1/3} T_\gamma \approx 1.945 K \rightarrow kT_\nu \approx 1.68 \cdot 10^{-4} eV$$

With a number density of:

$$n_f = \frac{3}{4}\frac{\varsigma(3)}{\pi^2} g_f T_f^3 \rightarrow n_{\nu_k,\bar{\nu}_k} \approx 0.1827 \cdot T_\nu^3 \approx 112 cm^{-3}$$

Neff

The relativistic neutrinos contribute to the present energy density of the Universe:

$$\rho_{rad} = \rho_\gamma + \rho_\nu = g_\gamma \left(\frac{\pi^2}{30}\right) T_\gamma^4 + g_\nu \left(\frac{\pi^2}{30}\right)\left(\frac{7}{8}\right) T_\nu^4$$

$$\rho_{rad} = \left(1 + \left(\frac{7}{8}\right)\left(\frac{4}{11}\right)^{\frac{4}{3}} \left(\frac{g_\nu}{g_\gamma}\right)\right) \rho_\gamma$$

We can introduce the effective number of relativistic degrees of freedom:

$$\rho_{rad} = \left[1 + \frac{7}{8}\left(\frac{4}{11}\right)^{4/3} N_{\rm eff}\right] \rho_\gamma$$

The expected value is $N_{eff} = 3.046$, if we assume standard electroweak interactions and three active massless neutrinos. The 0.046 takes into account effects for the non-instantaneous neutrino decoupling and neutrino flavour oscillations. (Mangano et al. 2005)

N_{eff}

Measuring $\Delta N_{eff} \equiv N_{eff} - 3.046$ we can constrain the dark radiation.

Increasing N_{eff} essentially increases the expansion rate H:

$$H^2 = \left(\frac{\dot{a}}{a}\right)^2 = H_0^2 \left(\frac{\Omega_r}{a^4} + \frac{\Omega_m}{a^3} + \frac{\Omega_k}{a^2} + \Omega_\Lambda\right)$$

So decrease the sound horizon at recombination,

$$r_s = \int_0^{t_*} c_s \, dt/a = \int_0^{a_*} \frac{c_s \, da}{a^2 H}$$

and the diffusion distance (damping scale):

$$r_d^2 = (2\pi)^2 \int_0^{a_*} \frac{da}{a^3 \sigma_T n_e H} \left[\frac{R^2 + \frac{16}{15}(1+R)}{6(1+R^2)}\right]$$

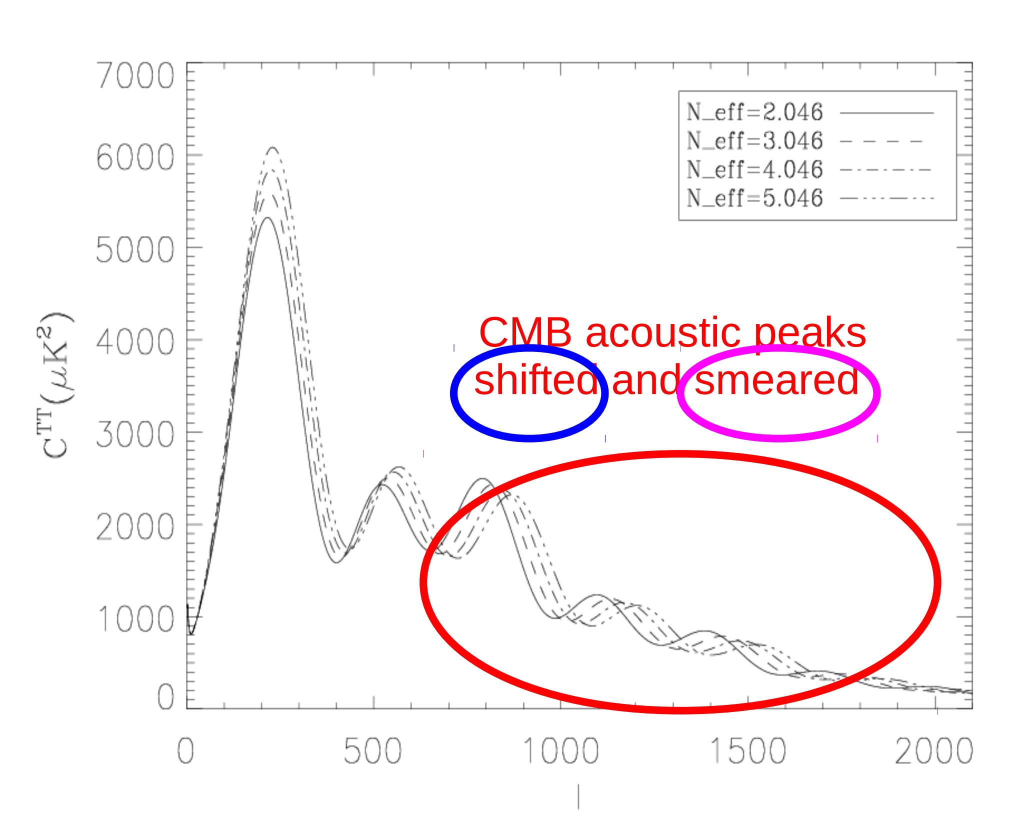

Probing the Neutrino Number with CMB data

Once the angular size of the sound horizon θ_s is fixed, we are fixing the angular scales of the acoustic peaks.

$$\theta_s = \frac{r_s}{D_A}$$

When we increase N_{eff}, we are increasing the angular scale of the diffusion length θ_d

$$\theta_d = \frac{r_d}{D_A}$$

and the result is an increasing of the damping in the small angular scale anisotropy.

$$\theta_d = \frac{r_d}{r_s}\theta_s \simeq \frac{\sqrt{H}^{-1}}{H^{-1}} = \sqrt{H}$$

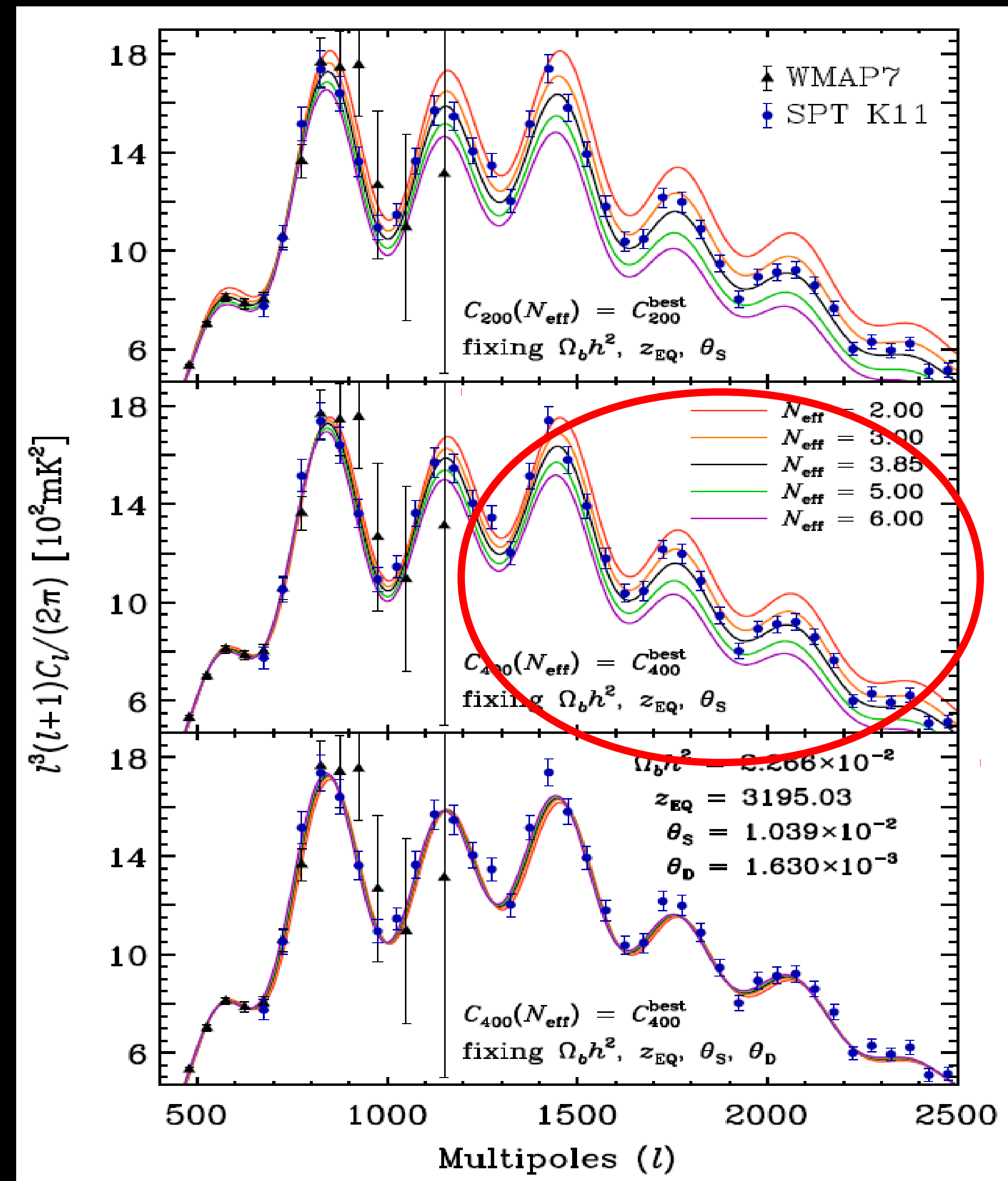

Hou et al., arXiv:1104.2333v2

The damping tail

The Planck satellite detected with higher precision the anisotropy damping tail, allowing to better constrain the parameters of new physics that affect it.

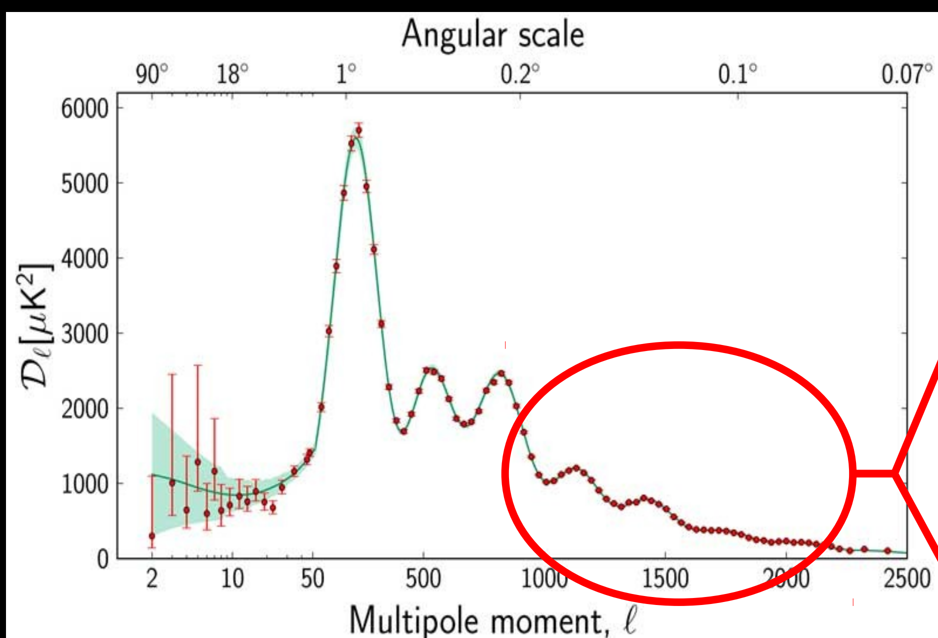

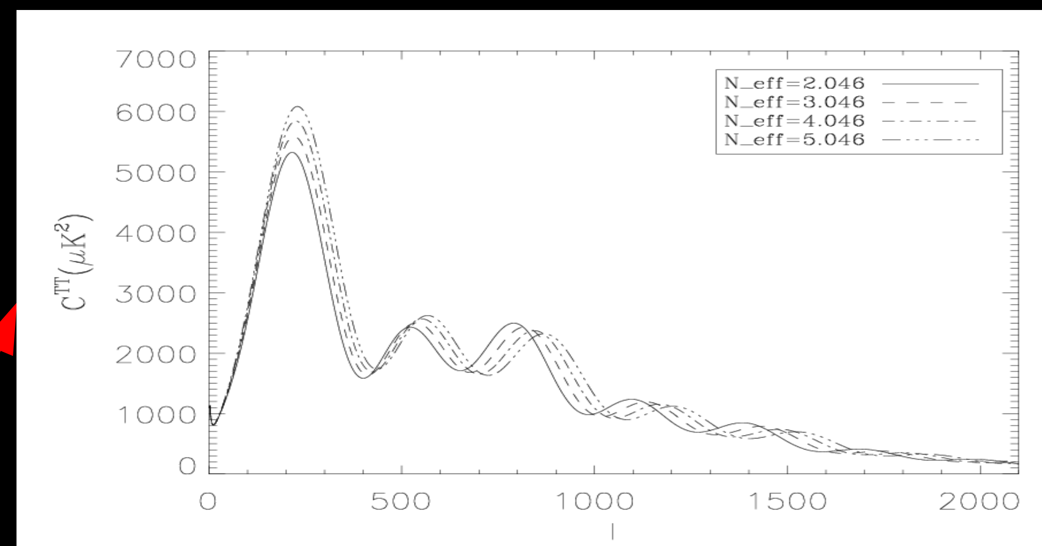

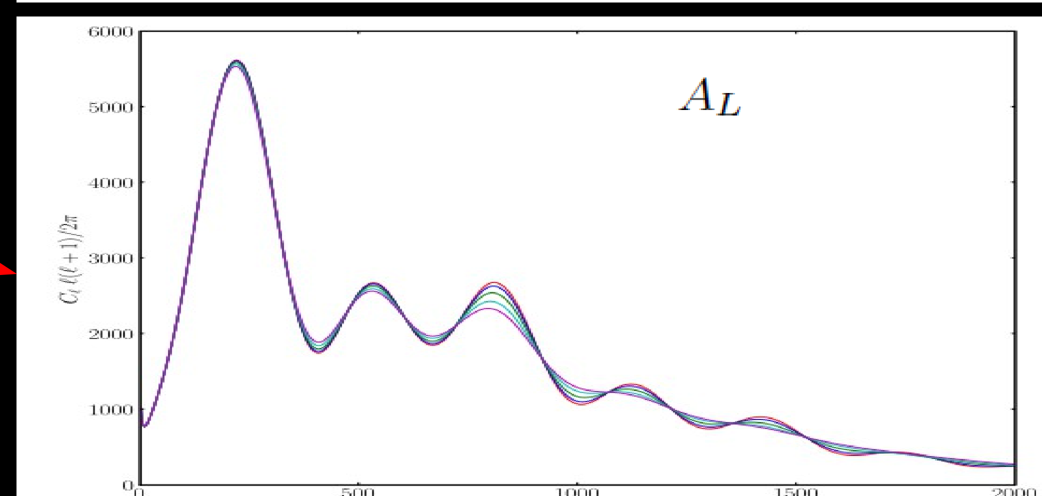

(E. Calabrese et al. 2008)

The lensing amplitude

The lensing amplitude A_L parameterizes the rescaling of the lensing potential $\phi(n)$, then the power spectrum of the lensing field:

$$C_\ell^{\phi\phi} \rightarrow A_L C_\ell^{\phi\phi}$$

The gravitational lensing deflects the photon path by a quantity defined by the gradient of the lensing potential $\phi(n)$, integrated along the line of sight n, remapping the temperature field.

Its effect on the power spectrum is the smoothing of the acoustic peaks, increasing A_L.

If A_L =1 then the theory is correct, else we have a new physics/systematics?

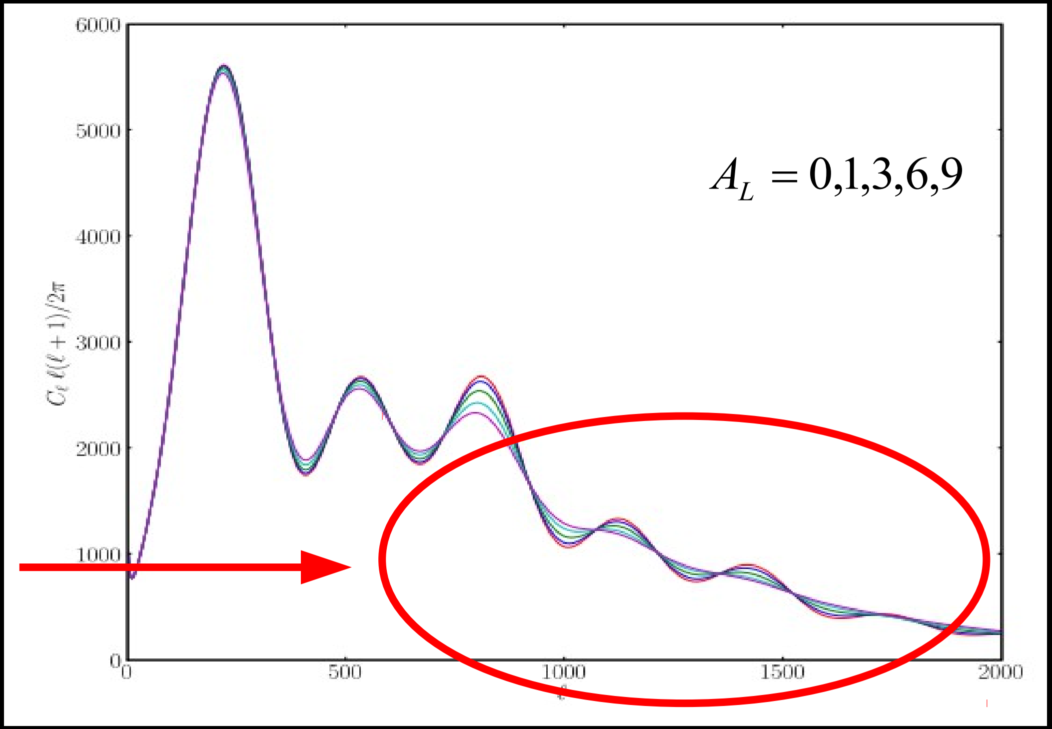

(E. Calabrese et al. 2008)

Pre-Planck constraints

Both N_{eff} and A_L affect the damping tail.

Before the release of the Planck data, ACT and SPT were in tension on constraining them.

Parameter	WMAP9 + SPT
$N_{\rm eff}$	3.72 ± 0.46
$A_{\rm L}$	0.85 ± 0.13

Parameter	WMAP9 + ACT
$N_{\rm eff}$	3.00 ± 0.61
$A_{\rm L}$	1.70 ± 0.37

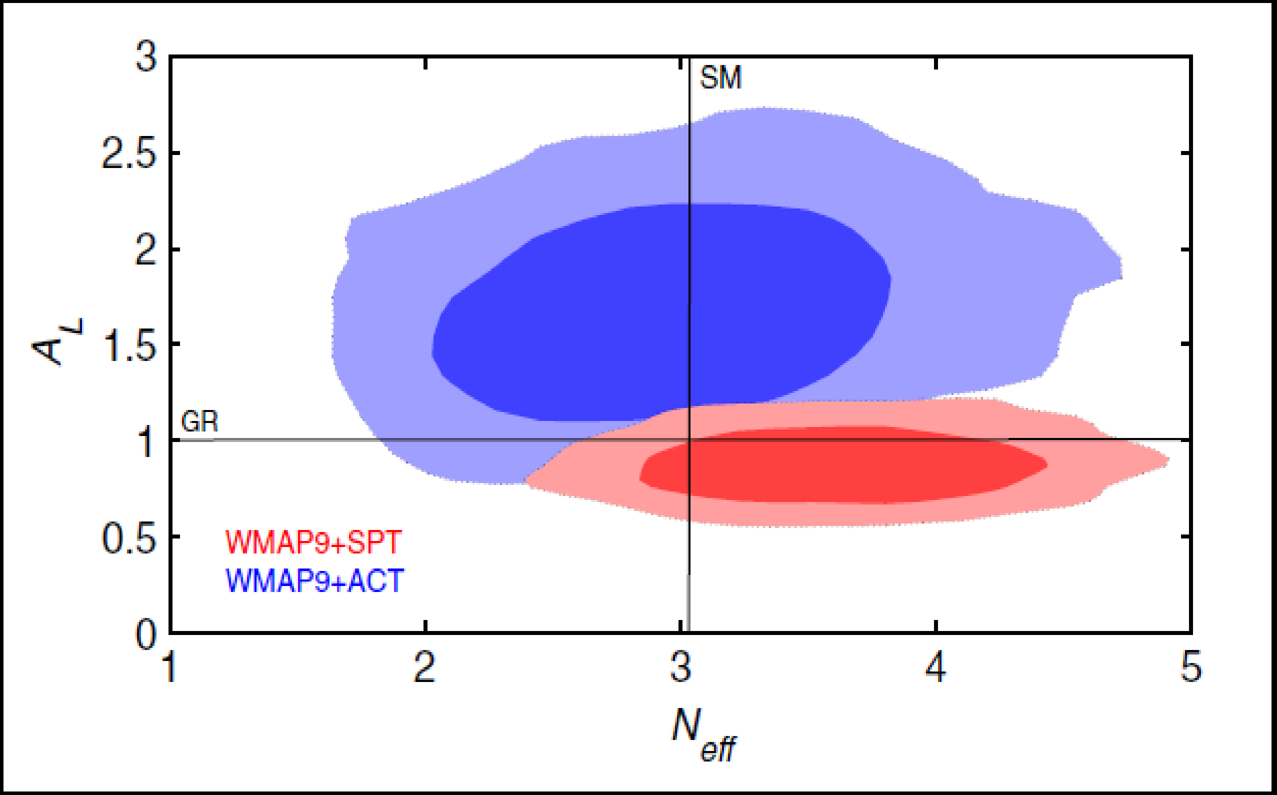

E. Di Valentino et al, Phys. Rev D, 88, 023501, 2013

E. D

What about Planck?

Planck+WP 2013 result does not solve the issue!

N_{eff} from Planck is in better agreement with SPT !

A_L from Planck is in better agreement with ACT !

$$N_{\rm eff} = 3.71 \pm 0.40$$

$$A_{\rm L} = 1.25 \pm 0.13$$

(68%; Planck+WP)

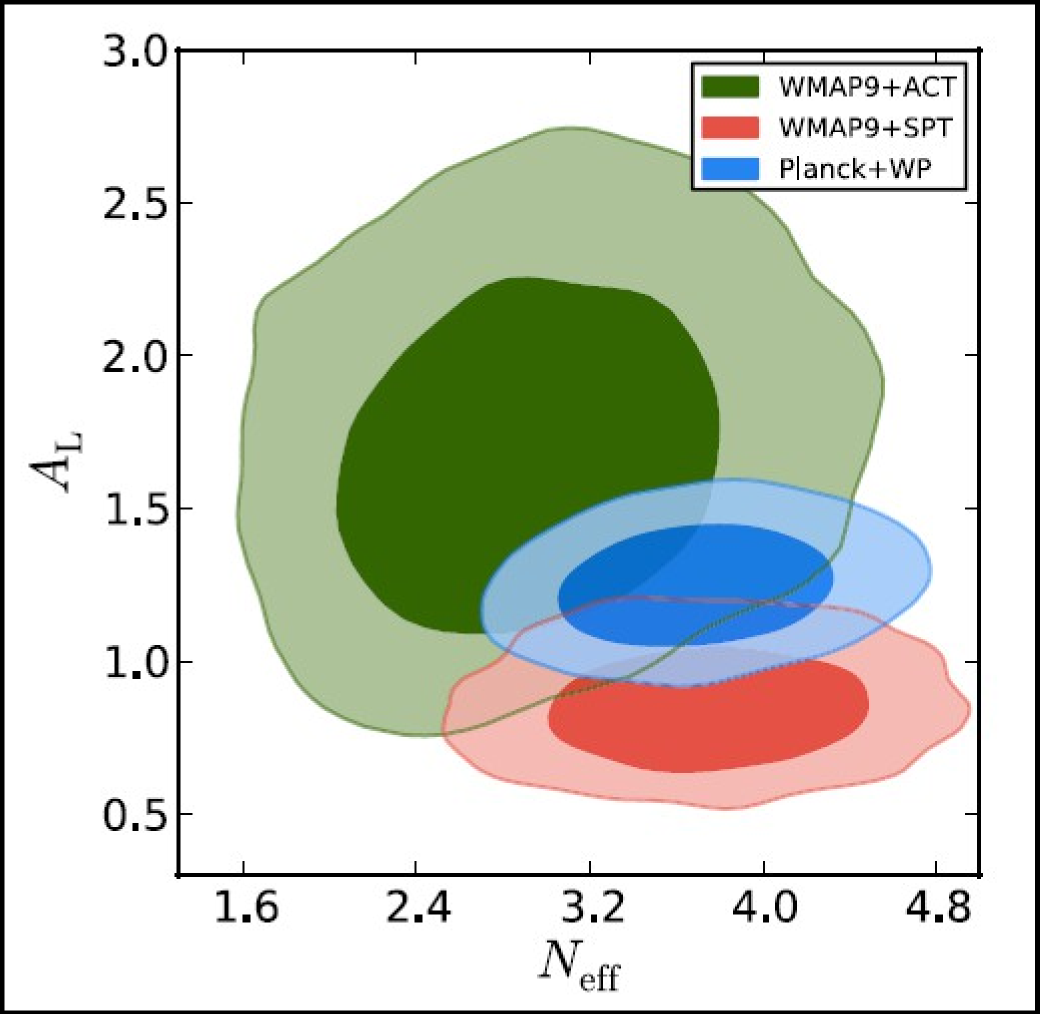

N. Said, E. Di Valentino, M. Gerbino, Phys. Rev D, 88, 023513, 2013

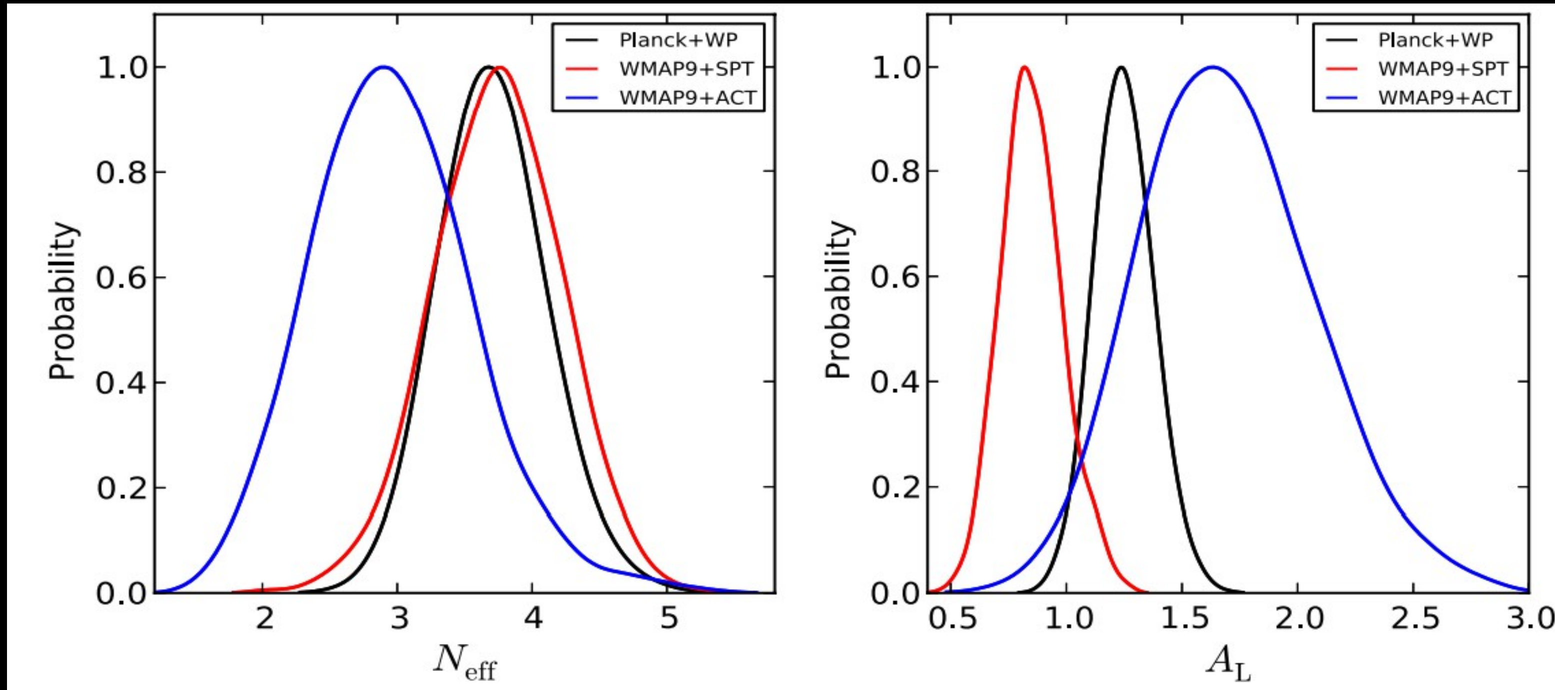

Parameter	Planck + WP	WMAP9 + SPT	WMAP9 + ACT
$\Omega_b h^2$	0.02306 ± 0.00051	0.02264 ± 0.00051	0.02295 ± 0.00052
$\Omega_c h^2$	0.1239 ± 0.0054	0.1232 ± 0.0080	0.112 ± 0.011
θ	1.04124 ± 0.00077	1.0415 ± 0.0012	1.0410 ± 0.0025
τ	0.095 ± 0.015	0.088 ± 0.014	0.090 ± 0.015
n_s	0.996 ± 0.018	0.982 ± 0.018	0.975 ± 0.019
$\log[10^{10} A_s]$	3.111 ± 0.034	3.169 ± 0.048	3.083 ± 0.044
$N_{\rm eff}$	3.71 ± 0.40	3.72 ± 0.46	3.00 ± 0.61
$A_{\rm L}$	1.25 ± 0.13	0.85 ± 0.13	1.70 ± 0.37
Ω_Λ	0.736 ± 0.022	0.736 ± 0.023	0.731 ± 0.025
t_0[Gyr]	13.08 ± 0.38	13.14 ± 0.43	13.74 ± 0.57
Ω_m	0.264 ± 0.022	0.264 ± 0.023	0.269 ± 0.025
H_0[km/s/Mpc]	74.9 ± 3.7	74.6 ± 3.7	70.9 ± 3.9

E. Di Valentino et al, Phys. Rev D, 88, 023501, 2013

N. Said, E. Di Valentino, M. Gerbino, Phys. Rev D, 88, 023513, 2013

E. Di Valentino et al, P

Parameter	WMAP7 + SPT [11]	WMAP9 + SPT [3]	WMAP7 + ACT [10]	WMAP9 + ACT [3]	Planck + WP [2]	PLANCK + WP
N_{eff}	3.62 ± 0.48	3.72 ± 0.46	2.78 ± 0.55	3.00 ± 0.61	3.51 ± 0.39	3.71 ± 0.40
A_{L}	1.00	0.85 ± 0.13	1.00	1.70 ± 0.37	1.00	1.25 ± 0.13
Parameter	WMAP7 + SPT [12]	WMAP9 + SPT [3]	WMAP7 + ACT [10]	WMAP9 + ACT [3]	Planck + WP [2]	PLANCK + WP
N_{eff}	3.046	3.72 ± 0.46	3.046	3.00 ± 0.61	3.046	3.71 ± 0.40
A_{L}	$0.86^{+0.15}_{-0.13}$	0.85 ± 0.13	1.70 ± 0.38	1.70 ± 0.37	$1.22^{+0.11}_{-0.13}$	1.25 ± 0.13

Allowing variations in A_L increases the mean value for N_{eff} by 5-10%.

There is a small, but not negligible correlation between the two parameters.

N. Said, E. Di Valentino, M. Gerbino, Phys. Rev D, 88, 023513, 2013

What about including HST or BAO data?

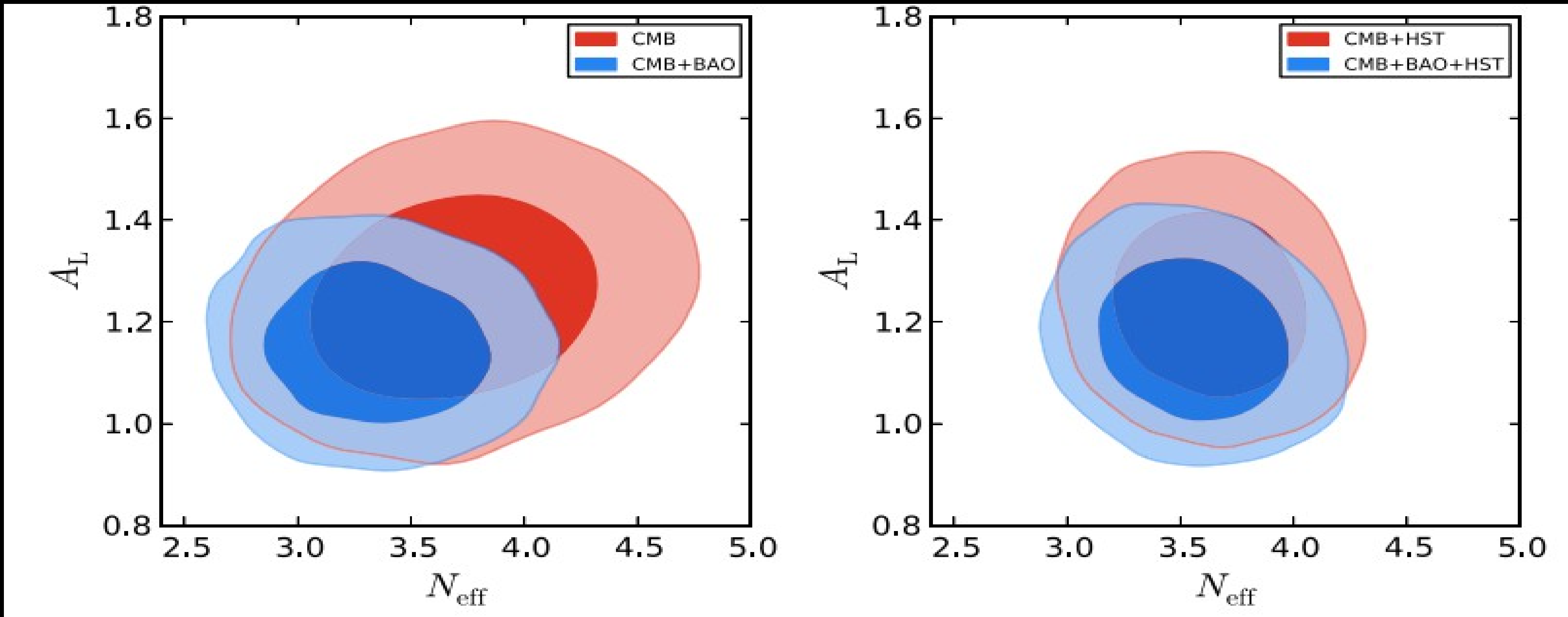

Results:

- HST brings N_{eff}>3.046 at more than 95% c.l.
- BAO brings N_{eff}=3.046 in between 68% c.l.
- BAO+HST gives N_{eff}>3.046 at about 95% c.l.

(HST wins over BAO)

We consider recent HST measurements (Riess et al. 2011) of H_0 = (73.8 ± 2.4) km/s/Mpc;

and for BAO surveys we include:

- SDSS-DR7 at redshift z=0.35
- SDSS-DR9 at z=0.57
- WiggleZ at z=0.44, 0.60, and 0.73.

N. Said, E. Di Valentino, M. Gerbino, Phys. Rev D, 88, 023513, 2013

What about H_0?

Moreover, analyzing the Planck data combined with the WMAP9 polarization data, only varying both N_{eff} and A_L we solve the tension to the value of the Hubble constant:

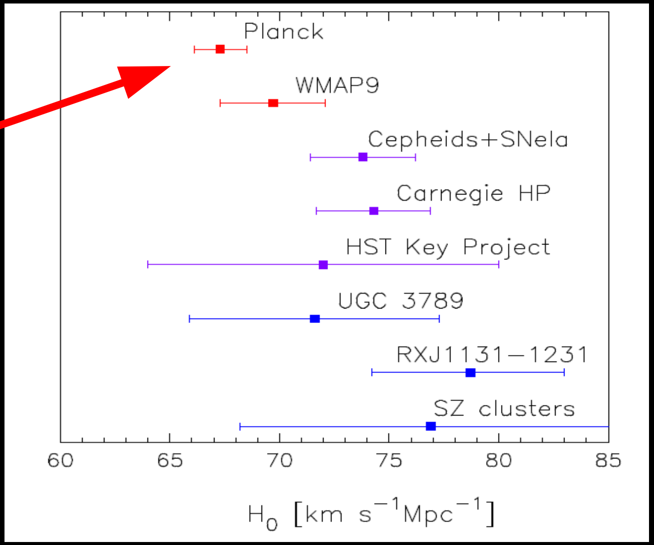

([Planck Collaboration], arXiv:1303.5076)

$$H_0 = (67.3 \pm 1.2)\ \mathrm{km\,s^{-1}\,Mpc^{-1}} \quad (68\%;\ \mathit{Planck}\text{+WP+highL}).$$

$$H_0 = (70.0 \pm 2.2)\ \mathrm{km\,s^{-1}\,Mpc^{-1}} \quad (68\%;\ \mathit{WMAP}\text{-9})$$

What about H_0?

Moreover, analyzing the Planck data combined with the WMAP9 polarization data, only varying both N_{eff} and A_L we solve the tension to the value of the Hubble constant:

Parameter	Planck+WP
$\Omega_b h^2$	0.02306 ± 0.00051
$\Omega_c h^2$	0.1239 ± 0.0054
θ	1.04124 ± 0.00077
τ	0.095 ± 0.015
n_s	0.996 ± 0.018
$log[10^{10} A_s]$	3.111 ± 0.034
$N_{\rm eff}$	3.71 ± 0.40
$A_{\rm L}$	1.25 ± 0.13
Ω_Λ	0.736 ± 0.022
$t_0[\rm Gyr]$	13.08 ± 0.38
Ω_m	0.264 ± 0.022
$H_0[\rm km/s/Mpc]$	74.9 ± 3.7

N. Said, E. Di Valentino, M. Gerbino, Phys. Rev D, 88, 023513, 2013

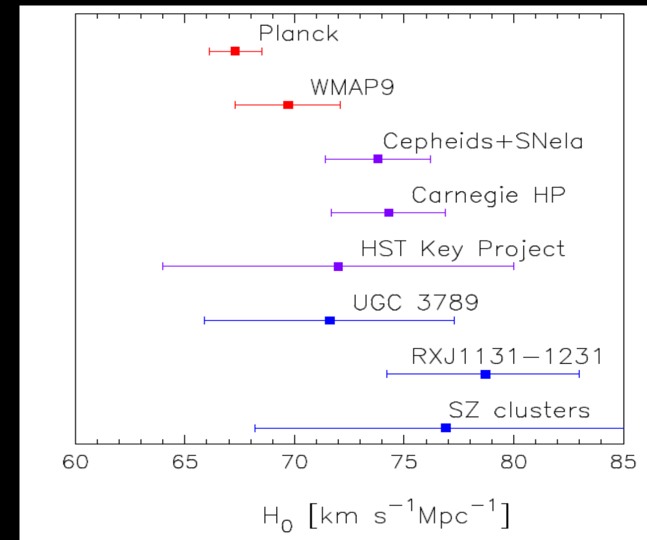

([Planck Collaboration], arXiv:1303.5076)

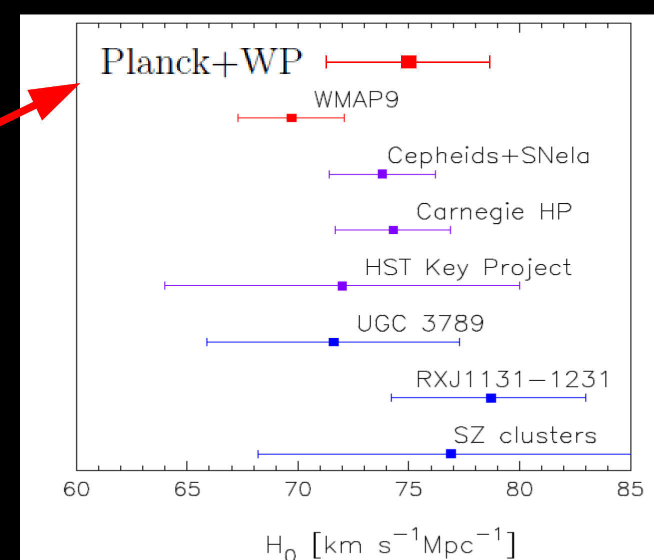

Sum of active neutrino masses

If the total neutrino mass is of the order of 1 eV, then the three active neutrinos are still relativistic at the time of recombination.

We expect the transition to the non-relativistic regime after the time of the photon decoupling.

Because the shape of the CMB spectrum is related mainly to the physical evolution before recombination, the effect of the neutrino mass, can appear through a modified background evolution and some secondary anisotropy corrections.

Sum of active neutrino masses

These neutrinos are radiation at the time of equality, and non-relativistic matter today.

Varying their total mass we vary:

- The redshift of the matter-to-radiation equality z_{eq};
- The amount of matter density today.

The impact on the CMB will be:

- The changing of the position and amplitude of the peaks;
- The slope of the low-l tail of the spectrum, due to the late ISW effect;
- The damping of the high-l tail, due to the lensing effect.

Sum of active neutrino masses

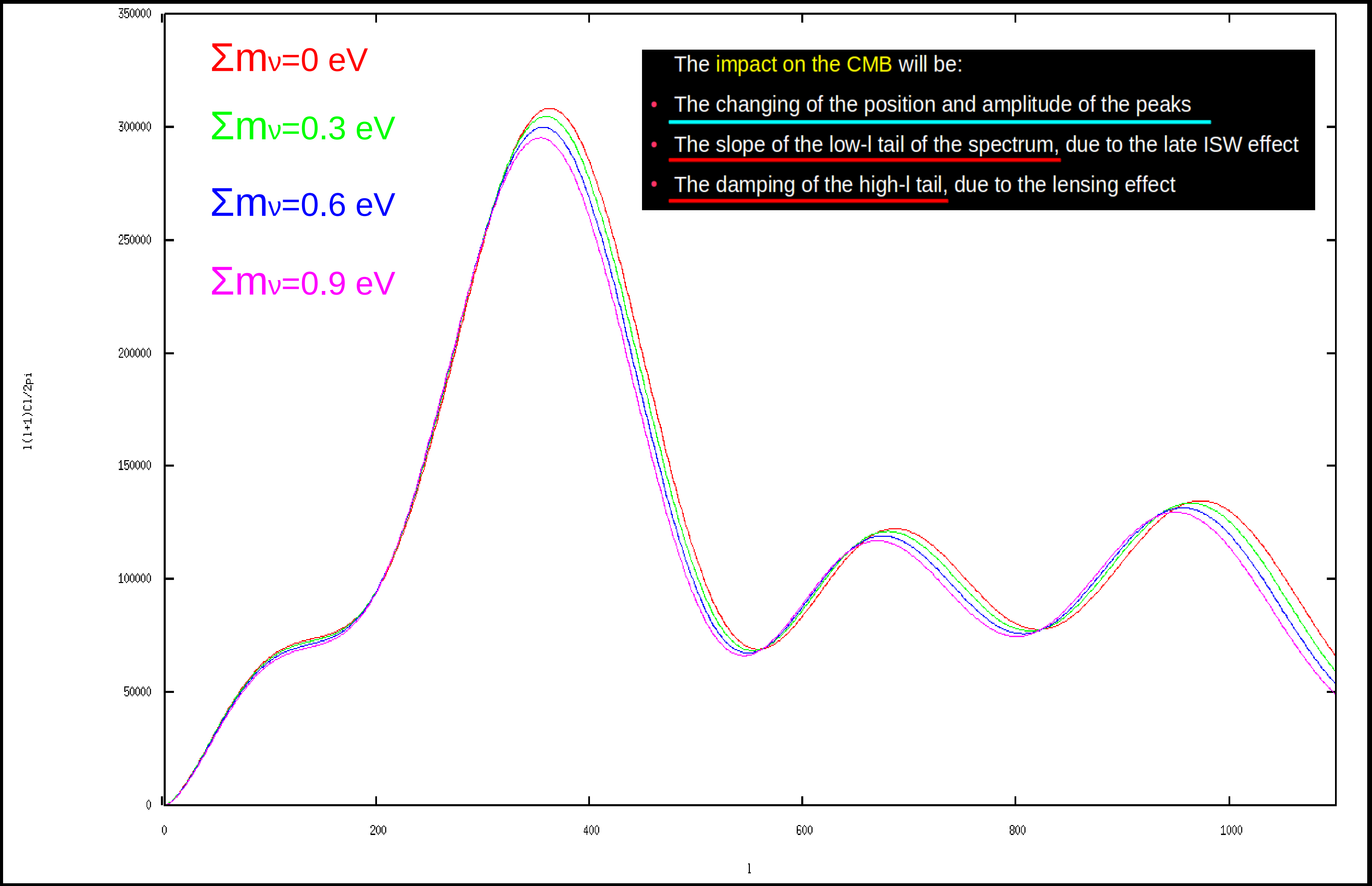

The matter power spectrum

The shape of the matter power spectrum is the key observable for costraining the neutrino masses with cosmological methods.

This is defined as the two-point correlation function of the non-relativistic matter fluctuation in Fourier space:

$$P(k,z) = \langle |\delta_{\rm m}(k,z)|^2 \rangle \quad \Rightarrow \quad \delta_{\rm m} = \frac{\sum_i \bar{\rho}_i \, \delta_i}{\sum_i \bar{\rho}_i}$$

The matter power spectrum is measured through the Large Scale Structure data.

The matter power spectrum

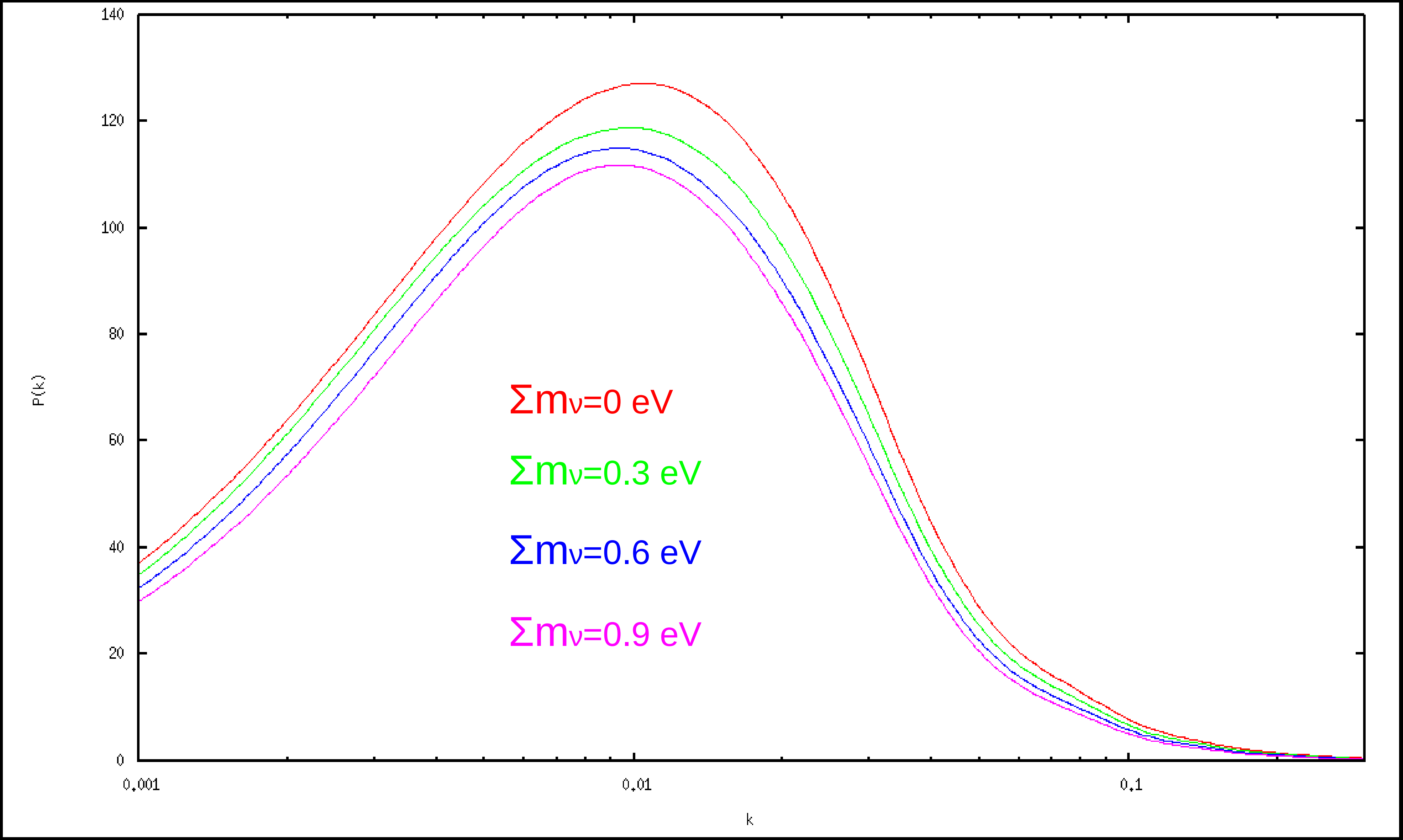

Imposing a flat Universe

New constraints

In E. Giusarma, E. Di Valentino, M. Lattanzi, A. Melchiorri and O. Mena, Phys. Rev. D90 (2014), 043507, we present up to date cosmological bounds on the sum of active neutrino masses as well as on extended cosmological scenarios with additional thermal relics, as thermal axions or sterile neutrino species.

Our analyses consider all the current available cosmological data in the beginning of year 2014:

CMB data:

- CMB temperature anisotropies measured by the Planck satellite (including information on the lensing potential);
- 9-year polarization data from WMAP;
- additional temperature data from high-resolution CMB experiments, ACT and SPT.

New constraints

In E. Giusarma, E. Di Valentino, M. Lattanzi, A. Melchiorri and O. Mena, Phys. Rev. D90 (2014), 043507, we present up to date cosmological bounds on the sum of active neutrino masses as well as on extended cosmological scenarios with additional thermal relics, as thermal axions or sterile neutrino species.

Our analyses consider all the current available cosmological data in the beginning of year 2014:

Large scale structure data:

All the available galaxy survey measurements in the form of Baryon Acoustic Oscillation (BAO) data:

- SDSS Data Release 7;
- WiggleZ survey;
- 6dF;
- BOSS Data Release 11 (DR11).

New constraints

In E. Giusarma, E. Di Valentino, M. Lattanzi, A. Melchiorri and O. Mena, Phys. Rev. D90 (2014), 043507, we present up to date cosmological bounds on the sum of active neutrino masses as well as on extended cosmological scenarios with additional thermal relics, as thermal axions or sterile neutrino species.

Our analyses consider all the current available cosmological data in the beginning of year 2014:

Large scale structure data:

The full matter power spectrum form in order to quantify the benefits of using shape measurements of the matter power spectrum versus geometrical BAO information:

- WiggleZ survey (WZ);

New constraints

In E. Giusarma, E. Di Valentino, M. Lattanzi, A. Melchiorri and O. Mena, Phys. Rev. D90 (2014), 043507, we present up to date cosmological bounds on the sum of active neutrino masses as well as on extended cosmological scenarios with additional thermal relics, as thermal axions or sterile neutrino species.

Our analyses consider all the current available cosmological data in the beginning of year 2014:

Additional datasets:

- Supernova luminosity distance measurements from the first 3 years of SNLS;
- Hubble costant measurements from HST: $H0 = (73.8 \pm 2.4)$ km/s/Mpc.

New constraints

In E. Giusarma, E. Di Valentino, M. Lattanzi, A. Melchiorri and O. Mena, Phys. Rev. D90 (2014), 043507, we present up to date cosmological bounds on the sum of active neutrino masses as well as on extended cosmological scenarios with additional thermal relics, as thermal axions or sterile neutrino species.

Our analyses consider all the current available cosmological data in the beginning of year 2014:

σ_8-Ω_m measurements:

- CFHTLens survey, through the amplitude and the shape of the weak lensing signal;
- The Planck Sunyaev-Zeldovich (SZ) selected clusters catalog, from the abundance of clusters as a function of the redshift.

Sum of active neutrino masses

	CMB+DR11	CMB+DR11 +HST	CMB+DR11 +WZ	CMB+DR11 +WZ+HST	CMB+ DR11 +WZ+BAO+HST	CMB+DR11 +BAO	CMB+DR11 +BAO+HST	CMB+ DR11 +BAO+SNLS
Σm_ν [eV]	< 0.25	< 0.22	< 0.25	< 0.23	< 0.24	< 0.26	< 0.22	< 0.23
SZ Clusters & CFHTLens								
Σm_ν [eV]	$0.30^{+0.12}_{-0.14}$	$0.25^{+0.12}_{-0.13}$	$0.27^{+0.14}_{-0.13}$	$0.25^{+0.10}_{-0.11}$	$0.26^{+0.18}_{-0.13}$	$0.29^{+0.13}_{-0.12}$	$0.24^{+0.10}_{-0.12}$	$0.27^{+0.12}_{-0.13}$
SZ Clusters								
Σm_ν [eV]	$0.30^{+0.12}_{-0.14}$	$0.25^{+0.13}_{-0.13}$	$0.27^{+0.12}_{-0.13}$	$0.24^{+0.10}_{-0.10}$	$0.25^{+0.17}_{-0.13}$	$0.29^{+0.13}_{-0.12}$	$0.23^{+0.10}_{-0.12}$	$0.27^{+0.11}_{-0.13}$
CFHTLens								
Σm_ν [eV]	< 0.33	< 0.28	< 0.30	< 0.27	< 0.28	< 0.33	< 0.27	< 0.30

TABLE II: 95% CL constraints on the sum of the neutrino masses, Σm_ν, from the different combinations of data sets explored here.

The most stringent bound on the sum of neutrino masses is considering CMB data + DR11 + HST

E. Giusarma, E. Di Valentino, M. Lattanzi, A. Melchiorri and O. Mena, Phys. Rev. D90 (2014), 043507

Sum of active neutrino masses

	CMB+DR11	CMB+DR11 +HST	CMB+DR11 +WZ	CMB+DR11 +WZ+HST	CMB+ DR11 +WZ+BAO+HST	CMB+DR11 +BAO	CMB+DR11 +BAO+HST	CMB+ DR11 +BAO+SNLS
Σm_ν [eV]	< 0.25	< 0.22	< 0.25	< 0.23	< 0.24	< 0.26	< 0.22	< 0.23
SZ Clusters & CFHTLens								
Σm_ν [eV]	$0.30^{+0.12}_{-0.14}$	$0.25^{+0.12}_{-0.13}$	$0.27^{+0.14}_{-0.13}$	$0.25^{+0.10}_{-0.11}$	$0.26^{+0.18}_{-0.13}$	$0.29^{+0.13}_{-0.12}$	$0.24^{+0.10}_{-0.12}$	$0.27^{+0.12}_{-0.13}$
SZ Clusters								
Σm_ν [eV]	$0.30^{+0.12}_{-0.14}$	$0.25^{+0.13}_{-0.13}$	$0.27^{+0.12}_{-0.13}$	$0.24^{+0.10}_{-0.10}$	$0.25^{+0.17}_{-0.13}$	$0.29^{+0.13}_{-0.12}$	$0.23^{+0.10}_{-0.12}$	$0.27^{+0.11}_{-0.13}$
CFHTLens								
Σm_ν [eV]	< 0.33	< 0.28	< 0.30	< 0.27	< 0.28	< 0.33	< 0.27	< 0.30

TABLE II: 95% CL constraints on the sum of the neutrino masses, Σm_ν, from the different combinations of data sets explored here.

A non zero value for the sum of the three active neutrino masses of 0.3 eV is signicantly favoured at more than 3σ when adding the constraints on σ_8 and Ω_m from the Planck Cluster catalog on galaxy number counts.

E. Giusarma, E. Di Valentino, M. Lattanzi, A. Melchiorri and O. Mena, Phys. Rev. D90 (2014), 043507

Sum of active neutrino masses

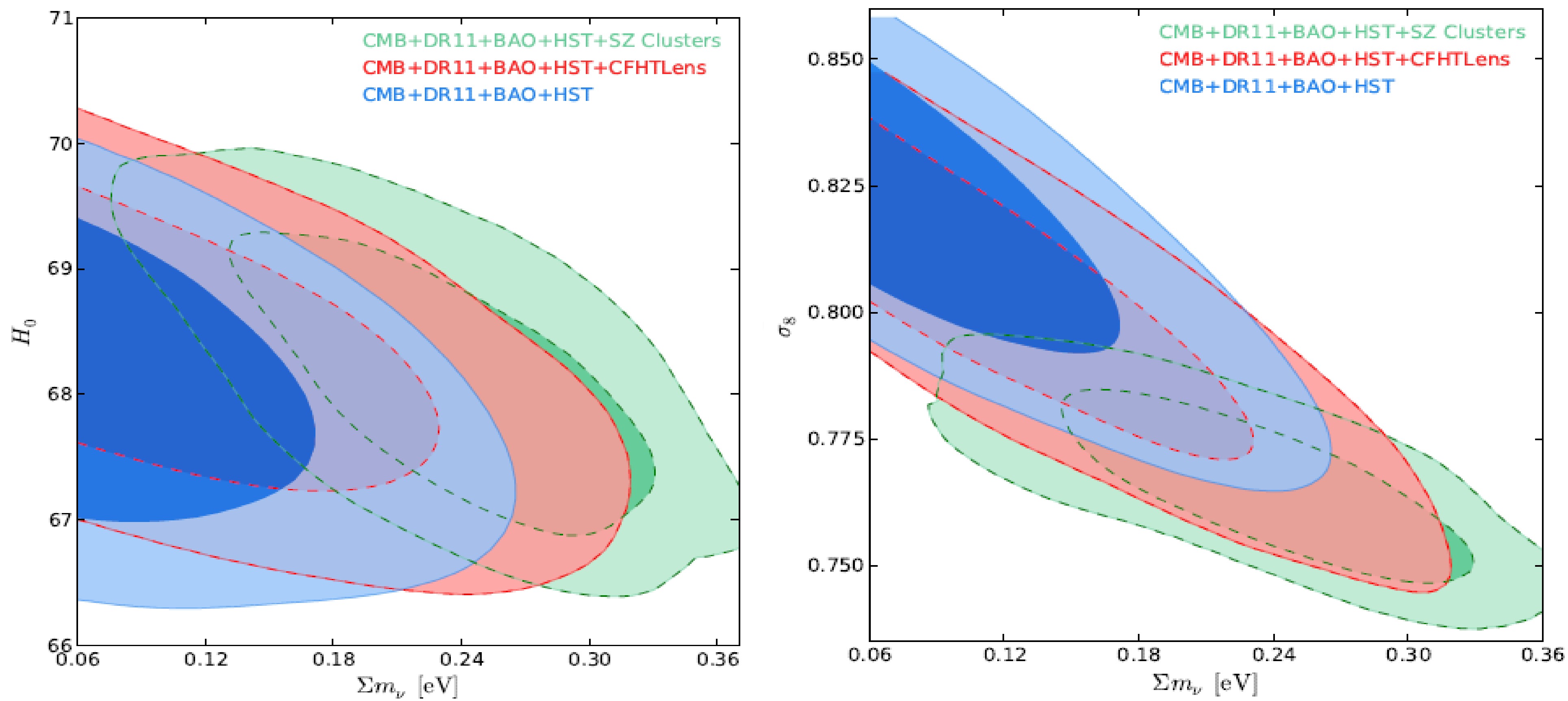

FIG. 1: Left panel: the blue contours show the 68% and 95% CL allowed regions from the combination of CMB data, BOSS DR11 BAO measurements, additional BAO measurements and a prior on the Hubble constant from HST in the ($\sum m_\nu$ (eV), H_0) plane. The red (green) contours depict the results when the $\sigma_8 - \Omega_m$ weak lensing (galaxy number counts) constraint is added in the analysis. Right panel: as in the left panel but in the ($\sum m_\nu$ (eV), σ_8) plane.

The power spectrum normalization σ_8 has smaller values when neutrinos are massive (due to the neutrino free streaming nature). These smaller values of σ_8 is preferred by galaxy cluster number counts.

E. Giusarma, E. Di Valentino, M. Lattanzi, A. Melchiorri and O. Mena, Phys. Rev. D90 (2014), 043507

Sum of active neutrino masses

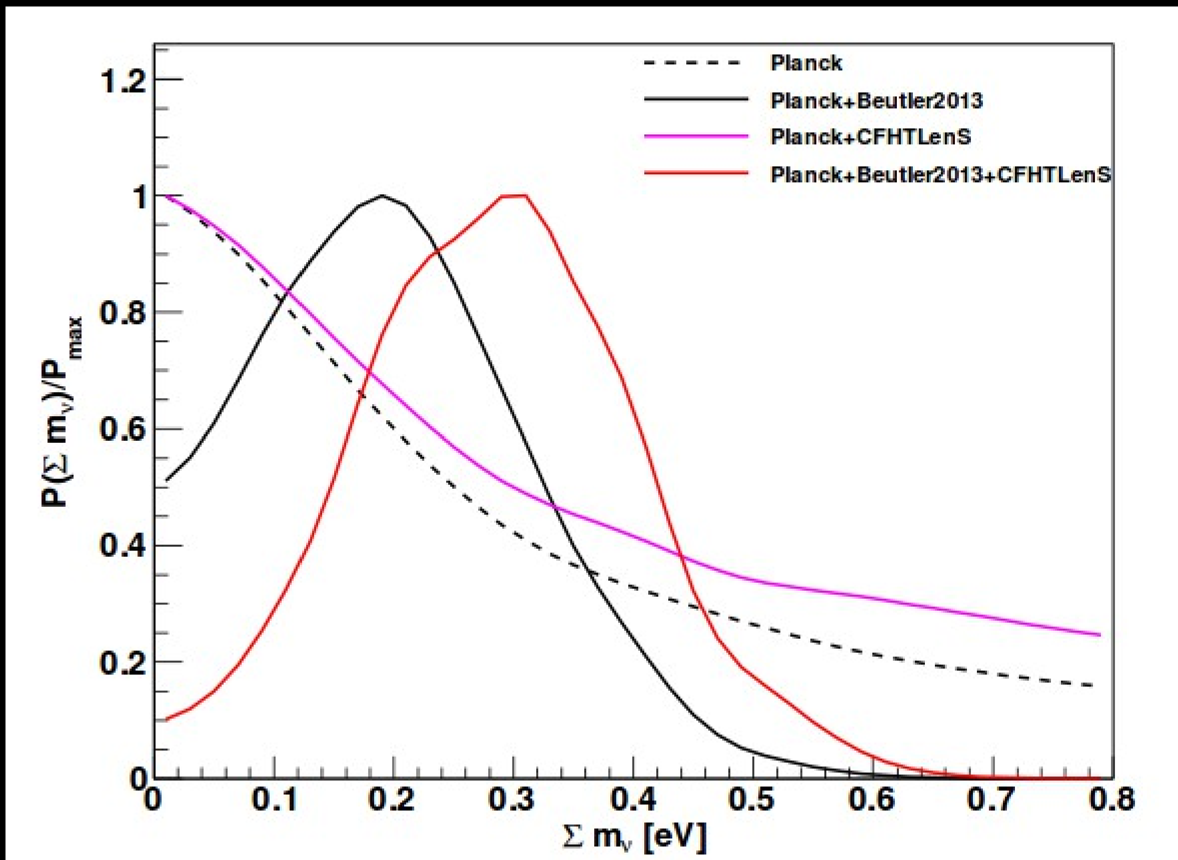

dataset(s)	$\sum m_\nu$ [eV] 68% c.l.	95% c.l.
Planck	< 0.41	< 0.95
Planck+CFHTLenS	< 0.51	< 1.0
Planck+Beutler2013	0.20 ± 0.13	< 0.40
Planck+Beutler2013+CFHTLenS	0.29 ± 0.13	$\boxed{0.29^{+0.29}_{-0.23}}$

Beutler et al., arXiv:1403.4599

The sum of the three active neutrino masses rules out the zero at more than 2σ also when are considered the BOSS CMASS DR 11 results of Beutler et al. (2013), which includes the measurement of the BAO scale, the Alcock-Paczynski effect and the signal of redshift-space distortions (RSD).

Sum of active neutrino masses

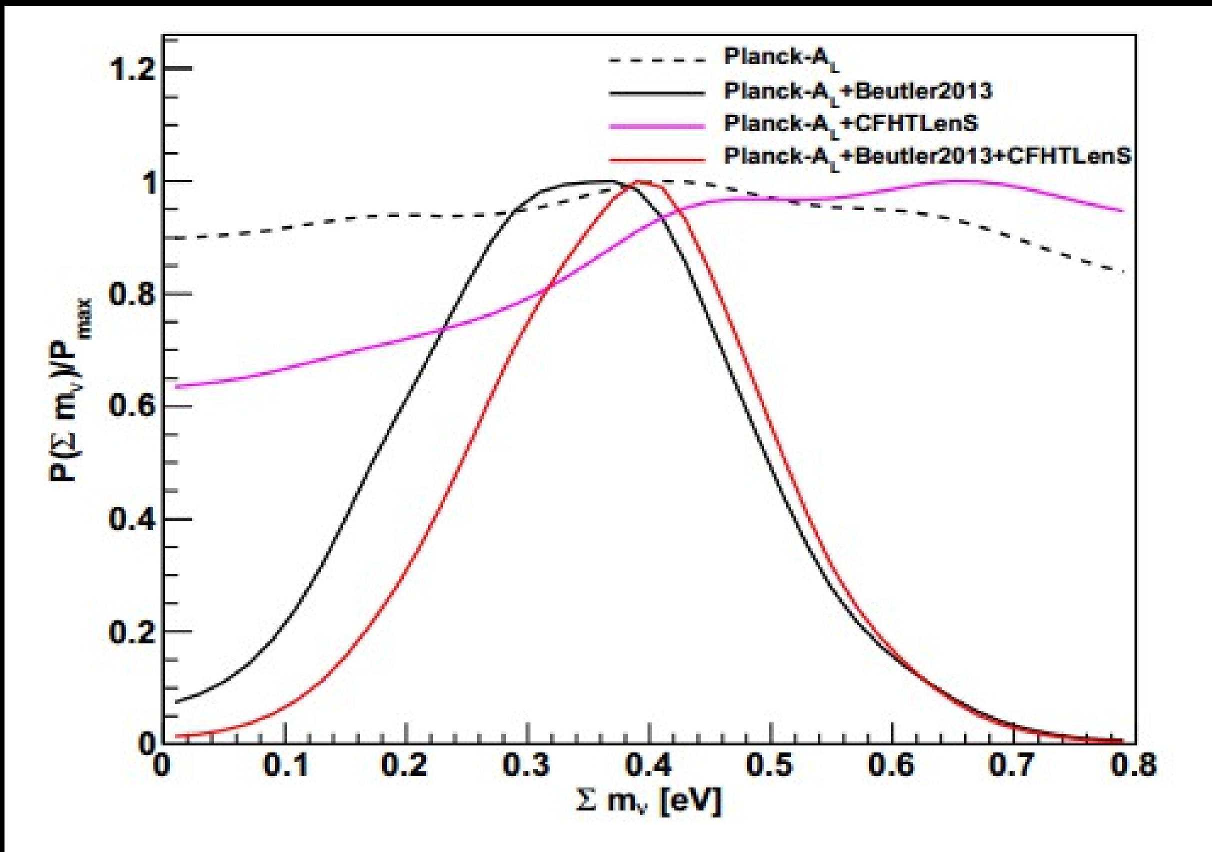

dataset(s)	$\sum m_\nu$ [eV] 68% c.l.	95% c.l.
Planck$-A_L$	< 0.71	< 1.2
Planck$-A_L$+CFHTLenS	$0.62^{+0.36}_{-0.50}$	< 1.3
Planck$-A_L$+Beutler2013	0.34 ± 0.14	$\boxed{0.34 \pm 0.26}$
Planck$-A_L$+Beutler2013+CFHTLenS	0.38 ± 0.11	$\boxed{0.38 \pm 0.24}$

Beutler et al., arXiv:1403.4599

...and the evidence for the sum of the three active neutrino masses becomes at more than 3σ when the Planck dataset is taken without the AL-lensing signal.

Sum of active neutrino masses

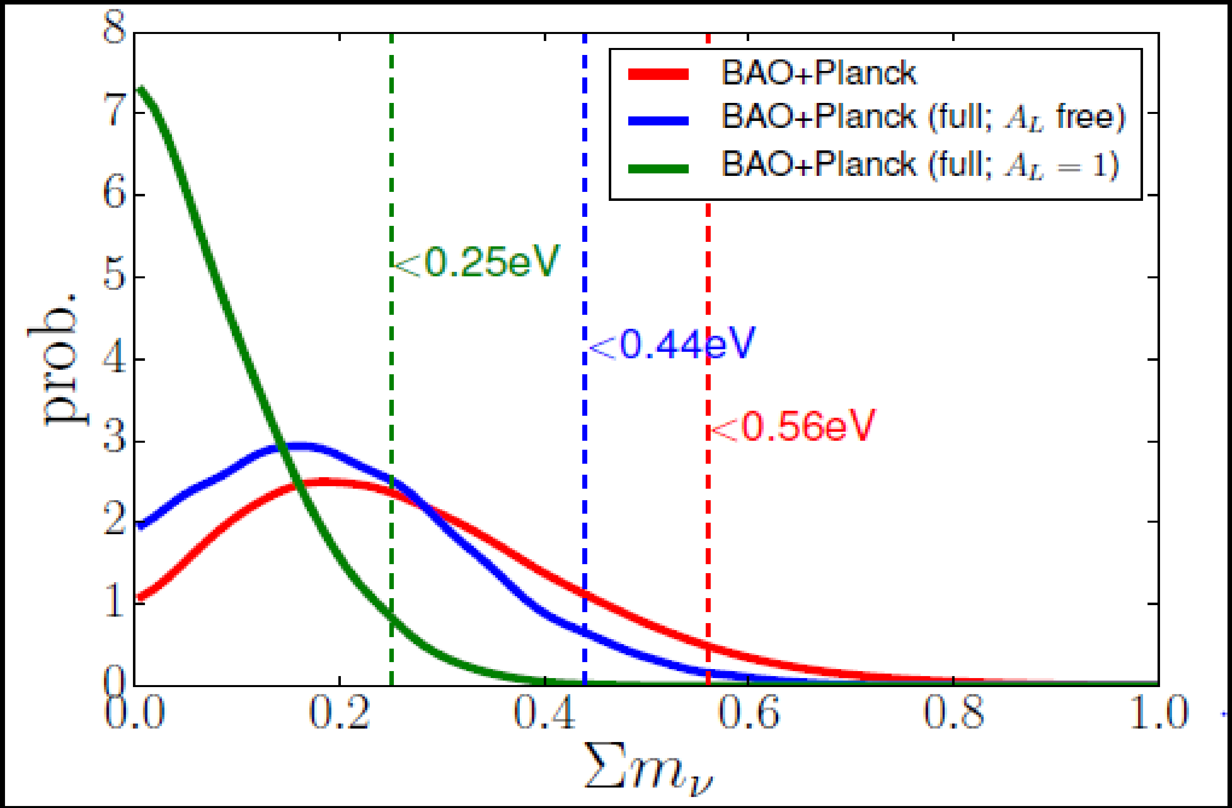

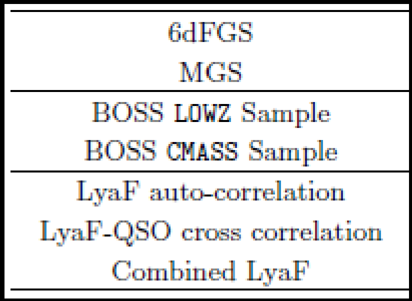

6dFGS
MGS
BOSS LOWZ Sample
BOSS CMASS Sample
LyaF auto-correlation
LyaF-QSO cross correlation
Combined LyaF

Aubourg et al., arXiv:1411.1074v1

The blue curve marginalizes over the parameter A_L, demonstrating that the difference between the green and red curves (where are taken from Planck data only geometrical informations) is driven mainly by the lensing amplitude information in the Planck data.

Neff

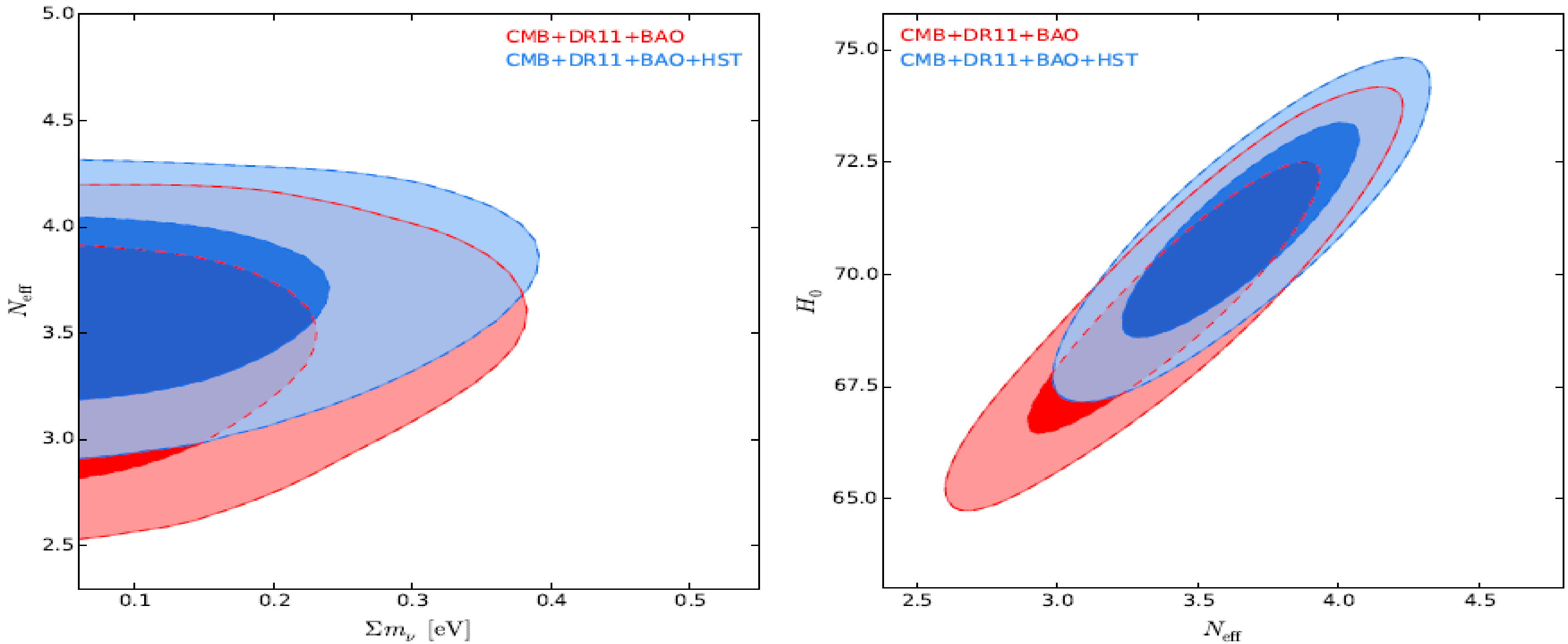

FIG. 3: Left panel: the red contours show the 68% and 95% CL allowed regions from the combination of CMB data, BOSS DR11 BAO measurements and additional BAO measurements in the ($\sum m_\nu$ (eV), $N_{\rm eff}$) plane. The blue contours depict the constraints after a prior on the Hubble constant from HST is added in the analysis. Right panel: as in the left panel but in the ($N_{\rm eff}$, H_0) plane.

When we vary also Neff, the bounds on the neutrino mass are less stringent, due to the large degeneracy between Σmν and Neff, in order to leave unchanged both the matter-radiation equality era and the location of the CMB acoustic peaks.

E. Giusarma, E. Di Valentino, M. Lattanzi, A. Melchiorri and O. Mena, Phys. Rev. D90 (2014), 043507

N_{eff}

	CMB+DR11	CMB+DR11 +HST	CMB+DR11 +WZ	CMB+DR11 +WZ+HST	CMB+DR11 +WZ+BAO+HST	CMB+DR11 +BAO	CMB+DR11 +BAO+HST	CMB+DR11 +BAO+SNLS
Σm_ν [eV]	< 0.31	< 0.31	< 0.32	< 0.34	< 0.34	< 0.31	< 0.31	< 0.29
$N_{\rm eff}$	$3.45^{+0.59}_{-0.54}$	$3.66^{+0.52}_{-0.49}$	$3.32^{+0.55}_{-0.62}$	$3.57^{+0.50}_{-0.48}$	$3.56^{+0.45}_{-0.49}$	$3.43^{+0.58}_{-0.59}$	$3.66^{+0.48}_{-0.47}$	$3.48^{+0.58}_{-0.56}$
SZ Clusters & CFHTLensing								
Σm_ν [eV]&	$0.37^{+0.24}_{-0.18}$	$0.37^{+0.20}_{-0.20}$	$0.32^{+0.19}_{-0.19}$	$0.35^{+0.16}_{-0.17}$	$0.37^{+0.26}_{-0.17}$	$0.32^{+0.18}_{-0.21}$	$0.37^{+0.18}_{-0.20}$	$0.32^{+0.15}_{-0.17}$
$N_{\rm eff}$	$3.32^{+0.53}_{-0.55}$	$3.54^{+0.48}_{-0.54}$	$3.24^{+0.58}_{-0.70}$	$3.56^{+0.59}_{-0.59}$	$3.56^{+1.09}_{-0.60}$	$3.17^{+0.64}_{-0.59}$	$3.54^{+60}_{-0.62}$	$3.25^{+0.47}_{-0.43}$
SZ Clusters								
Σm_ν [eV]	$0.37^{+0.24}_{-0.19}$	$0.36^{+0.18}_{-0.18}$	$0.32^{+0.19}_{-0.19}$	$0.35^{+0.17}_{-0.16}$	$0.36^{+0.26}_{-0.18}$	$0.32^{+0.18}_{-0.20}$	$0.37^{+0.18}_{-0.21}$	$0.32^{+0.15}_{-0.16}$
$N_{\rm eff}$	$3.33^{+0.55}_{-0.53}$	$3.55^{+0.51}_{-0.58}$	$3.25^{+0.57}_{-0.68}$	$3.56^{+0.59}_{-0.58}$	$3.55^{+0.65}_{-0.59}$	$3.18^{+0.63}_{-0.59}$	$3.54^{+0.62}_{-0.59}$	$3.25^{+0.49}_{-0.44}$

When we vary also N_{eff}, the bounds on the neutrino mass are less stringent, due to the large degeneracy between Σm_ν and N_{eff}, in order to leave unchanged both the matter-radiation equality era and the location of the CMB acoustic peaks.

E. Giusarma, E. Di Valentino, M. Lattanzi, A. Melchiorri and O. Mena, Phys. Rev. D90 (2014), 043507

N_{eff}

	CMB+DR11	CMB+DR11 +HST	CMB+DR11 +WZ	CMB+DR11 +WZ+HST	CMB+DR11 +WZ+BAO+HST	CMB+DR11 +BAO	CMB+DR11 +BAO+HST	CMB+DR11 +BAO+SNLS
Σm_ν [eV]	< 0.31	< 0.31	< 0.32	< 0.34	< 0.34	< 0.31	< 0.31	< 0.29
$N_{\rm eff}$	$3.45^{+0.59}_{-0.54}$	$3.66^{+0.52}_{-0.49}$	$3.32^{+0.55}_{-0.62}$	$3.57^{+0.50}_{-0.48}$	$3.56^{+0.45}_{-0.49}$	$3.43^{+0.58}_{-0.59}$	$3.66^{+0.48}_{-0.47}$	$3.48^{+0.58}_{-0.56}$
SZ Clusters & CFHTLensing								
Σm_ν [eV]&	$0.37^{+0.24}_{-0.18}$	$0.37^{+0.20}_{-0.20}$	$0.32^{+0.19}_{-0.19}$	$0.35^{+0.16}_{-0.17}$	$0.37^{+0.26}_{-0.17}$	$0.32^{+0.18}_{-0.21}$	$0.37^{+0.18}_{-0.20}$	$0.32^{+0.15}_{-0.17}$
$N_{\rm eff}$	$3.32^{+0.53}_{-0.55}$	$3.54^{+0.48}_{-0.54}$	$3.24^{+0.58}_{-0.70}$	$3.56^{+0.59}_{-0.59}$	$3.56^{+1.09}_{-0.60}$	$3.17^{+0.64}_{-0.59}$	$3.54^{+60}_{-0.62}$	$3.25^{+0.47}_{-0.43}$
SZ Clusters								
Σm_ν [eV]	$0.37^{+0.24}_{-0.19}$	$0.36^{+0.18}_{-0.18}$	$0.32^{+0.19}_{-0.19}$	$0.35^{+0.17}_{-0.16}$	$0.36^{+0.26}_{-0.18}$	$0.32^{+0.18}_{-0.20}$	$0.37^{+0.18}_{-0.21}$	$0.32^{+0.15}_{-0.16}$
$N_{\rm eff}$	$3.33^{+0.55}_{-0.53}$	$3.55^{+0.51}_{-0.58}$	$3.25^{+0.57}_{-0.68}$	$3.56^{+0.59}_{-0.58}$	$3.55^{+0.65}_{-0.59}$	$3.18^{+0.63}_{-0.59}$	$3.54^{+0.62}_{-0.59}$	$3.25^{+0.49}_{-0.44}$

Since HST measurements point to a higher H_0 value, a larger value of N_{eff} will be favoured by data, which also implies a higher neutrino mass bound due to the strong Σm_ν - N_{eff} degeneracy.

E. Giusarma, E. Di Valentino, M. Lattanzi, A. Melchiorri and O. Mena, Phys. Rev. D90 (2014), 043507

N_{eff}

	CMB+DR11	CMB+DR11 +HST	CMB+DR11 +WZ	CMB+DR11 +WZ+HST	CMB+DR11 +WZ+BAO+HST	CMB+DR11 +BAO	CMB+DR11 +BAO+HST	CMB+DR11 +BAO+SNLS
Σm_ν [eV]	< 0.31	< 0.31	< 0.32	< 0.34	< 0.34	< 0.31	< 0.31	< 0.29
$N_{\rm eff}$	$3.45^{+0.59}_{-0.54}$	$3.66^{+0.52}_{-0.49}$	$3.32^{+0.55}_{-0.62}$	$3.57^{+0.50}_{-0.48}$	$3.56^{+0.45}_{-0.49}$	$3.43^{+0.58}_{-0.59}$	$3.66^{+0.48}_{-0.47}$	$3.48^{+0.58}_{-0.56}$
SZ Clusters & CFHTLensing								
Σm_ν [eV]&	$0.37^{+0.24}_{-0.18}$	$0.37^{+0.20}_{-0.20}$	$0.32^{+0.19}_{-0.19}$	$0.35^{+0.16}_{-0.17}$	$0.37^{+0.26}_{-0.17}$	$0.32^{+0.18}_{-0.21}$	$0.37^{+0.18}_{-0.20}$	$0.32^{+0.15}_{-0.17}$
$N_{\rm eff}$	$3.32^{+0.53}_{-0.55}$	$3.54^{+0.48}_{-0.54}$	$3.24^{+0.58}_{-0.70}$	$3.56^{+0.59}_{-0.59}$	$3.56^{+1.09}_{-0.60}$	$3.17^{+0.64}_{-0.59}$	$3.54^{+60}_{-0.62}$	$3.25^{+0.47}_{-0.43}$
SZ Clusters								
Σm_ν [eV]	$0.37^{+0.24}_{-0.19}$	$0.36^{+0.18}_{-0.18}$	$0.32^{+0.19}_{-0.19}$	$0.35^{+0.17}_{-0.16}$	$0.36^{+0.26}_{-0.18}$	$0.32^{+0.18}_{-0.20}$	$0.37^{+0.18}_{-0.21}$	$0.32^{+0.15}_{-0.16}$
$N_{\rm eff}$	$3.33^{+0.55}_{-0.53}$	$3.55^{+0.51}_{-0.58}$	$3.25^{+0.57}_{-0.68}$	$3.56^{+0.59}_{-0.58}$	$3.55^{+0.65}_{-0.59}$	$3.18^{+0.63}_{-0.59}$	$3.54^{+0.62}_{-0.59}$	$3.25^{+0.49}_{-0.44}$

A non zero value for the sum of the three active neutrino masses of 0.3 eV is signicantly favoured at more than 3σ when adding the constraints on σ_8 and Ω_m from the Planck Cluster catalog on galaxy number counts.

E. Giusarma, E. Di Valentino, M. Lattanzi, A. Melchiorri and O. Mena, Phys. Rev. D90 (2014), 043507

The effective sterile neutrino mass

We can constrain also the effective sterile neutrino mass with N_{eff}. Their relationship is strongly model dependent, but fixed the model we can infer the physical mass of the particle.

Contribution of the sterile neutrino when it is massless.

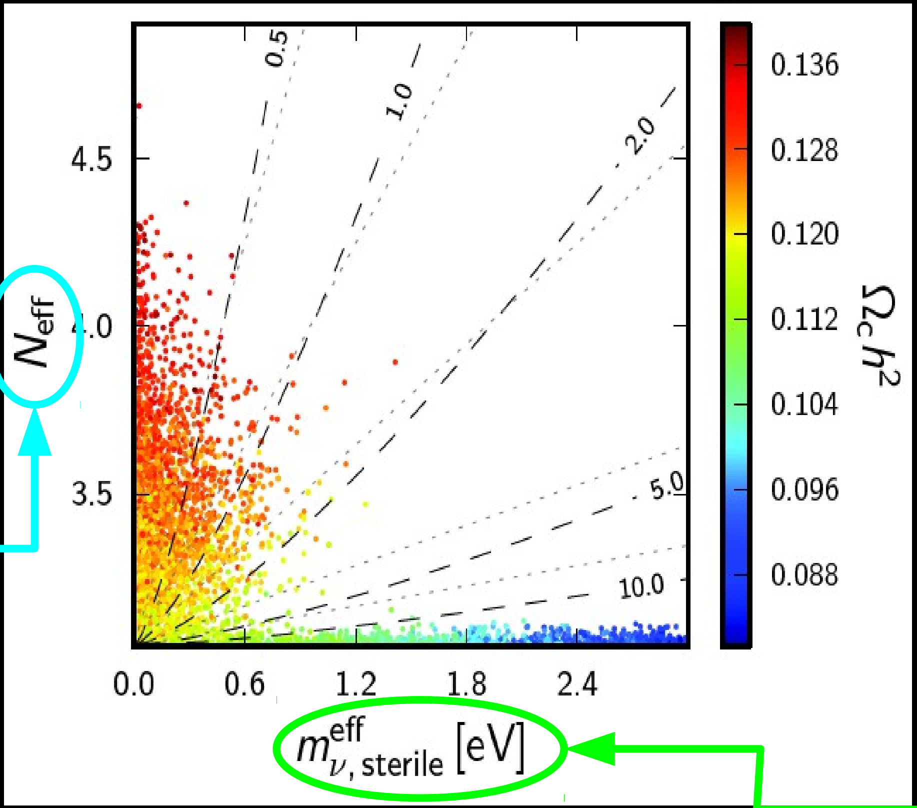

Thermally distributed

$$m^{eff}_{\nu,\,sterile} = (T_s/T_\nu)^3 m^{thermal}_{sterile} = (\Delta N_{eff})^{3/4} m^{thermal}_{sterile}$$

Distributed proportionally to active neutrinos (Dodelson-Widrow model)

$$m^{eff}_{\nu,\,sterile} = \chi_s m^{DW}_{sterile}$$

$$\Delta N_{eff} = \chi_s$$

Contribution of the sterile neutrino when it is massive.

$$\left.\begin{array}{r} N_{eff} < 3.91 \\ m^{eff}_{\nu,\,sterile} < 0.59\,\mathrm{eV} \end{array}\right\} \quad (95\%;\ \mathrm{CMB\ for}\ m^{thermal}_{sterile} < 10\,\mathrm{eV})$$

(Planck collaboration 2013)

The effective sterile neutrino mass

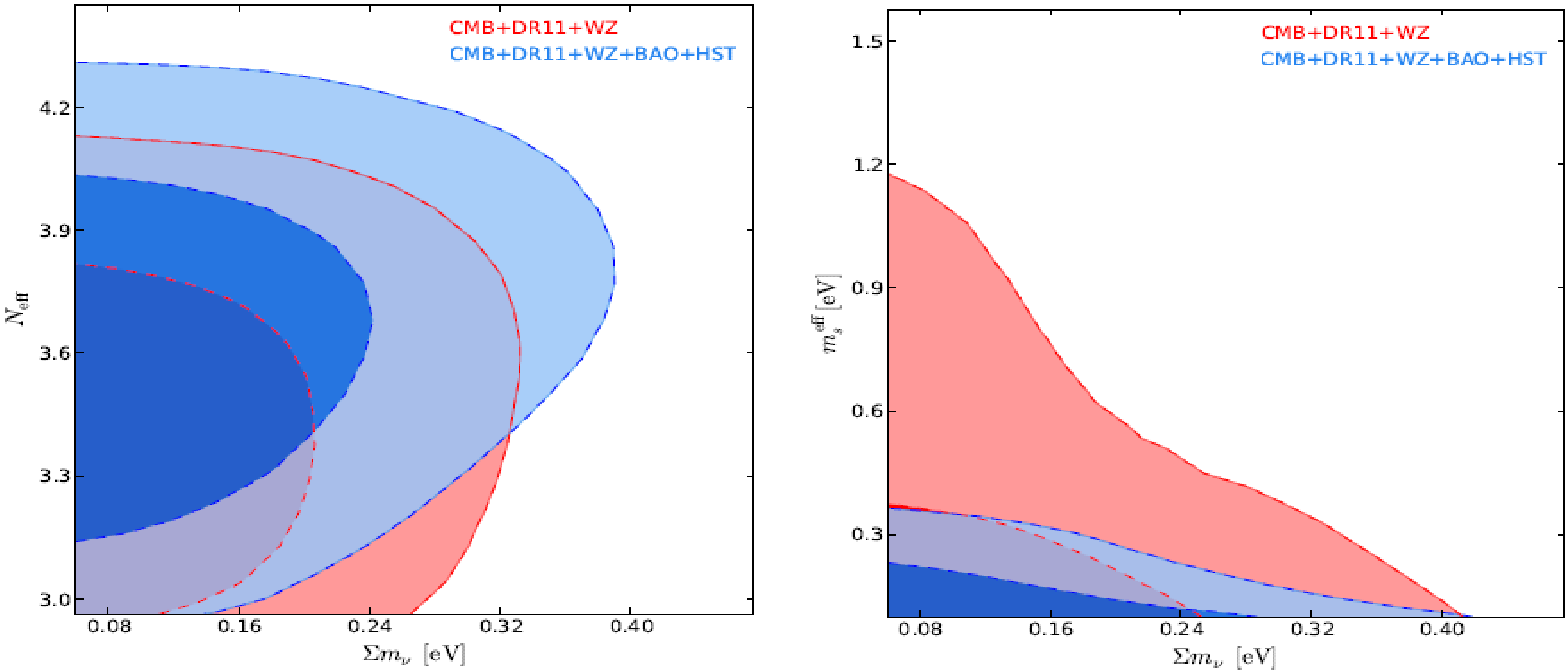

FIG. 4: Left panel: the red contours show the 68% and 95% CL allowed regions from the combination of CMB data, BOSS DR11 BAO measurements and WiggleZ full shape power spectrum measurements in the ($\sum m_\nu$ (eV), $N_{\rm eff}$) plane. The blue contours depict the constraints after a prior on the Hubble constant from HST and the remaining BAO data are added in the analysis. Right panel: as in the left panel but in the ($\sum m_\nu$ (eV), $m_s^{\rm eff}$ (eV)) plane.

When we consider the massive sterile neutrinos, $N_{\rm eff}$ and the sum of the three active neutrinos masses are slightly larger. This is due to the fact that either are positively correlated with the sterile neutrinos.

E. Giusarma, E. Di Valentino, M. Lattanzi, A. Melchiorri and O. Mena, Phys. Rev. D90 (2014), 043507

The effective sterile neutrino mass

	CMB+DR11	CMB+DR11 +HST	CMB+DR11 +WZ	CMB+DR11 +WZ+HST	CMB+DR11 +WZ+BAO+HST	CMB+DR11 +BAO	CMB+DR11 +BAO+HST	CMB+DR11 +BAO+SNLS
Σm_ν [eV]	< 0.28	< 0.27	< 0.28	< 0.30	< 0.31	< 0.30 [a]	< 0.29	< 0.26
$m_s^{\rm eff}$ [eV]	< 0.29	< 0.28	< 0.60	< 0.28	< 0.25	< 0.27 [a]	< 0.28	< 0.31
$N_{\rm eff}$	< 4.01	$3.73^{+0.51}_{-0.51}$	< 3.89	< 4.06	$3.64^{+0.48}_{-0.48}$	$3.57^{+0.50}_{-0.50}$ [a]	< 4.16	< 4.02
SZ Clusters& CFHTLens								
Σm_ν [eV]	< 0.40	< 0.43	< 0.36	< 0.41	< 0.43	< 0.43	< 0.39	< 0.37
$m_s^{\rm eff}$ [eV]	< 0.50	< 0.48	< 1.37	< 0.39	< 0.34	< 0.49	< 0.59	< 0.59
$N_{\rm eff}$	< 3.90	$3.67^{+0.49}_{-0.55}$	< 3.77	< 4.08	$3.67^{+0.51}_{-0.45}$	$3.47^{+0.51}_{-0.39}$	< 4.01	< 3.85
SZ Clusters								
Σm_ν [eV]	< 0.40	< 0.42	< 0.36	< 0.41	< 0.42	< 0.41	< 0.39	< 0.38
$m_s^{\rm eff}$ [eV]	< 0.49	< 0.48	< 1.36	< 0.39	< 0.34	< 0.49	< 0.53	< 0.59
$N_{\rm eff}$	< 3.90	$3.66^{+0.49}_{-0.55}$	< 3.77	< 4.06	$3.66^{+0.50}_{-0.45}$	$3.46^{+0.41}_{-0.38}$	< 4.02	< 3.85

When we consider the massive sterile neutrinos, $N_{\rm eff}$ and the sum of the three active neutrinos masses are slightly larger.

E. Giusarma, E. Di Valentino, M. Lattanzi, A. Melchiorri and O. Mena, Phys. Rev. D90 (2014), 043507

The effective sterile neutrino mass

	CMB+DR11	CMB+DR11 +HST	CMB+DR11 +WZ	CMB+DR11 +WZ+HST	CMB+DR11 +WZ+BAO+HST	CMB+DR11 +BAO	CMB+DR11 +BAO+HST	CMB+DR11 +BAO+SNLS
Σm_ν [eV]	< 0.28	< 0.27	< 0.28	< 0.30	< 0.31	< 0.30 [a]	< 0.29	< 0.26
$m_s^{\rm eff}$ [eV]	< 0.29	< 0.28	< 0.60	< 0.28	< 0.25	< 0.27 [a]	< 0.28	< 0.31
$N_{\rm eff}$	< 4.01	$3.73^{+0.51}_{-0.51}$	< 3.89	< 4.06	$3.64^{+0.48}_{-0.48}$	$3.57^{+0.50}_{-0.50}$ [a]	< 4.16	< 4.02
SZ Clusters& CFHTLens								
Σm_ν [eV]	< 0.40	< 0.43	< 0.36	< 0.41	< 0.43	< 0.43	< 0.39	< 0.37
$m_s^{\rm eff}$ [eV]	< 0.50	< 0.48	< 1.37	< 0.39	< 0.34	< 0.49	< 0.59	< 0.59
$N_{\rm eff}$	< 3.90	$3.67^{+0.49}_{-0.55}$	< 3.77	< 4.08	$3.67^{+0.51}_{-0.45}$	$3.47^{+0.51}_{-0.39}$	< 4.01	< 3.85
SZ Clusters								
Σm_ν [eV]	< 0.40	< 0.42	< 0.36	< 0.41	< 0.42	< 0.41	< 0.39	< 0.38
$m_s^{\rm eff}$ [eV]	< 0.49	< 0.48	< 1.36	< 0.39	< 0.34	< 0.49	< 0.53	< 0.59
$N_{\rm eff}$	< 3.90	$3.66^{+0.49}_{-0.55}$	< 3.77	< 4.06	$3.66^{+0.50}_{-0.45}$	$3.46^{+0.41}_{-0.38}$	< 4.02	< 3.85

When we add the HST measurements of the Hubble costant, $N_{\rm eff}$ rules out the standard value at more than 2σ.

E. Giusarma, E. Di Valentino, M. Lattanzi, A. Melchiorri and O. Mena, Phys. Rev. D90 (2014), 043507

The effective sterile neutrino mass

	CMB+DR11	CMB+DR11 +HST	CMB+DR11 +WZ	CMB+DR11 +WZ+HST	CMB+DR11 +WZ+BAO+HST	CMB+DR11 +BAO	CMB+DR11 +BAO+HST	CMB+DR11 +BAO+SNLS
Σm_ν [eV]	< 0.28	< 0.27	< 0.28	< 0.30	< 0.31	< 0.30 [a]	< 0.29	< 0.26
$m_s^{\rm eff}$ [eV]	< 0.29	< 0.28	< 0.60	< 0.28	< 0.25	< 0.27 [a]	< 0.28	< 0.31
$N_{\rm eff}$	< 4.01	$3.73^{+0.51}_{-0.51}$	< 3.89	< 4.06	$3.64^{+0.48}_{-0.48}$	$3.57^{+0.50}_{-0.50}$ [a]	< 4.16	< 4.02
SZ Clusters& CFHTLens								
Σm_ν [eV]	< 0.40	< 0.43	< 0.36	< 0.41	< 0.43	< 0.43	< 0.39	< 0.37
$m_s^{\rm eff}$ [eV]	< 0.50	< 0.48	< 1.37	< 0.39	< 0.34	< 0.49	< 0.59	< 0.59
$N_{\rm eff}$	< 3.90	$3.67^{+0.49}_{-0.55}$	< 3.77	< 4.08	$3.67^{+0.51}_{-0.45}$	$3.47^{+0.51}_{-0.39}$	< 4.01	< 3.85
SZ Clusters								
Σm_ν [eV]	< 0.40	< 0.42	< 0.36	< 0.41	< 0.42	< 0.41	< 0.39	< 0.38
$m_s^{\rm eff}$ [eV]	< 0.49	< 0.48	< 1.36	< 0.39	< 0.34	< 0.49	< 0.53	< 0.59
$N_{\rm eff}$	< 3.90	$3.66^{+0.49}_{-0.55}$	< 3.77	< 4.06	$3.66^{+0.50}_{-0.45}$	$3.46^{+0.41}_{-0.38}$	< 4.02	< 3.85

When adding the constraints on σ_8 and Ω_m from the Planck Cluster catalog on galaxy number counts, we haven't in this case that Σm_ν is different to zero.

E. Giusarma, E. Di Valentino, M. Lattanzi, A. Melchiorri and O. Mena, Phys. Rev. D90 (2014), 043507

The effective sterile neutrino mass

	$\nu\Lambda$CDM–CL
$\Delta N_{\rm eff}$	$\boxed{0.62 \pm 0.28}$
m_s [eV]	$\boxed{0.48 \pm 0.15}$
r	–
$100\Omega_b h^2$	2.267 ± 0.028
$\Omega_c h^2$	0.122 ± 0.005
$100\theta_{\rm MC}$	1.041 ± 0.001
τ	0.096 ± 0.014
$\ln(10^{10}A_s)$	3.107 ± 0.031
n_s	0.985 ± 0.012
h	0.70 ± 0.01
S_8	0.81 ± 0.01

$\nu\Lambda$CDM	ΛCDM$+N_{\rm eff}+m_s$
CL	C$+H_0+$BAO$+$Clusters

Dvorkin et al., arXiv:1403.8049

If the BOSS DR11 dataset is removed, and the sum of the three active neutrinos masses is fixed to 0.06eV, we can find evidence simultaneously for $N_{\rm eff}$ and the mass of the sterile neutrino.

Axions

The most elegant and promising solution of the so-called *strong CP problem* in Quantum Chromodynamics (QCD) was provided by Peccei and Quinn, adding a new global $U(1)_{PQ}$ symmetry. This is spontaneously broken at an energy scale f_a, generating a new spinless particle, the axion. The axion can be copiously produced in the universe's early stages, both via thermal and non-thermal processes.

- Thermal axions with sub-eV masses contribute to the hot dark matter component of the universe, as neutrinos, and we have updated the cosmological limits on their properties in E. Giusarma, E. Di Valentino, M. Lattanzi, A. Melchiorri and O. Mena, Phys. Rev. D90 (2014), 043507.
- Axion-like particles produced non-thermally, instead were postulated as natural candidates for the cold dark matter component, and we put this "axion dark matter" (ADM) scenario under scrutiny using the most recent cosmological data in E. Di Valentino, E. Giusarma, M. Lattanzi, A. Melchiorri and O. Mena, Phys. Rev. D90 (2014), 043534.

Thermal Axions

Thermal axions with sub-eV masses contribute to the hot dark matter component of the universe, so to the extra radiation component at the BBN period, by an amount given by:

$$\Delta N_{\rm eff} = \frac{4}{7}\left(\frac{3}{2}\frac{n_a}{n_\nu}\right)^{4/3}$$

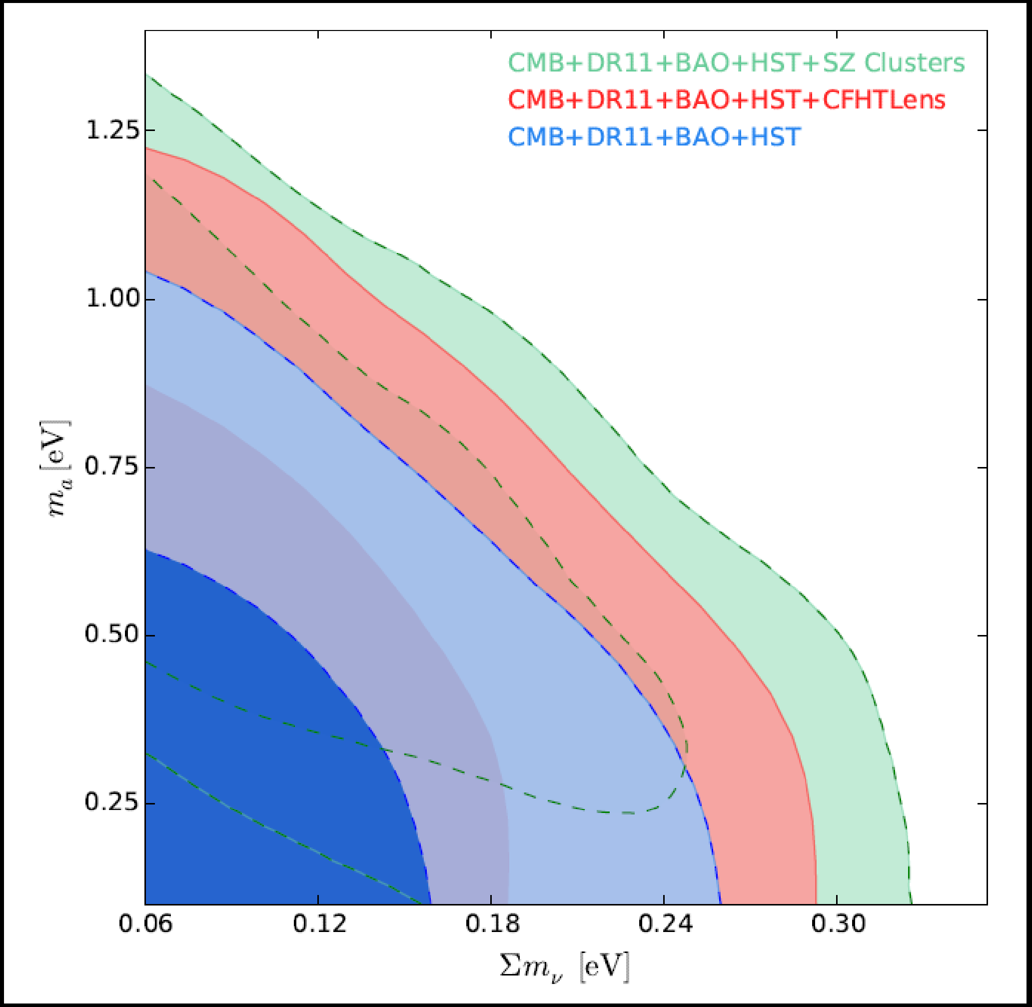

E. Giusarma, E. Di Valentino, M. Lattanzi, A. Melchiorri and O. Mena, Phys. Rev. D90 (2014), 043507

Thermal Axions

	CMB+DR11	CMB+DR11 +HST	CMB+DR11 +WZ	CMB+DR11 +WZ+HST	CMB+DR11 +WZ+BAO+HST	CMB+DR11 +BAO	CMB+DR11 +BAO+HST	CMB+DR11 +BAO+SNLS
Σm_ν [eV]	< 0.24	< 0.21	< 0.24	< 0.22	< 0.21	< 0.23	< 0.20	< 0.22
m_a [eV]	< 0.79	< 0.77	< 0.65	< 0.62	< 0.59	< 0.74	< 0.75	< 0.76
SZ Clusters & CFHTLensing								
Σm_ν [eV]	< 0.36	< 0.27	$0.21^{+013}_{-0.13}$	< 0.32	< 0.30	< 0.31	< 0.28	< 0.31
m_a [eV]	< 1.08	< 1.09	< 0.88	< 0.81	< 0.77	< 1.12	$0.63^{+0.47}_{-0.49}$	$0.58^{+0.50}_{-0.48}$
SZ Clusters								
Σm_ν [eV]	< 0.36	< 0.27	$0.20^{+013}_{-0.14}$	< 0.32	< 0.30	< 0.31	< 0.27	< 0.31
m_a [eV]	< 1.07	< 1.07	< 0.87	< 0.81	< 0.77	< 1.10	$0.62^{+0.46}_{-0.48}$	$0.57^{+0.50}_{-0.47}$

For these datasets we have only upper limits for the axion mass and the neutrino masses.

E. Giusarma, E. Di Valentino, M. Lattanzi, A. Melchiorri and O. Mena, Phys. Rev. D90 (2014), 043507

Thermal Axions

	CMB+DR11	CMB+DR11 +HST	CMB+DR11 +WZ	CMB+DR11 +WZ+HST	CMB+DR11 +WZ+BAO+HST	CMB+DR11 +BAO	CMB+DR11 +BAO+HST	CMB+DR11 +BAO+SNLS
Σm_ν [eV]	< 0.24	< 0.21	< 0.24	< 0.22	< 0.21	< 0.23	< 0.20	< 0.22
m_a [eV]	< 0.79	< 0.77	< 0.65	< 0.62	< 0.59	< 0.74	< 0.75	< 0.76
SZ Clusters & CFHTLensing								
Σm_ν [eV]	< 0.36	< 0.27	$0.21^{+013}_{-0.13}$	< 0.32	< 0.30	< 0.31	< 0.28	< 0.31
m_a [eV]	< 1.08	< 1.09	< 0.88	< 0.81	< 0.77	< 1.12	$0.63^{+0.47}_{-0.49}$	$0.58^{+0.50}_{-0.48}$
SZ Clusters								
Σm_ν [eV]	< 0.36	< 0.27	$0.20^{+013}_{-0.14}$	< 0.32	< 0.30	< 0.31	< 0.27	< 0.31
m_a [eV]	< 1.07	< 1.07	< 0.87	< 0.81	< 0.77	< 1.10	$0.62^{+0.46}_{-0.48}$	$0.57^{+0.50}_{-0.47}$

For these datasets there is an evidence at more than 2σ for an axion mass of 0.6eV

E. Giusarma, E. Di Valentino, M. Lattanzi, A. Melchiorri and O. Mena, Phys. Rev. D90 (2014), 043507

Thermal Axions

	CMB+DR11	CMB+DR11 +HST	CMB+DR11 +WZ	CMB+DR11 +WZ+HST	CMB+DR11 +WZ+BAO+HST	CMB+DR11 +BAO	CMB+DR11 +BAO+HST	CMB+DR11 +BAO+SNLS
Σm_ν [eV]	< 0.24	< 0.21	< 0.24	< 0.22	< 0.21	< 0.23	< 0.20	< 0.22
m_a [eV]	< 0.79	< 0.77	< 0.65	< 0.62	< 0.59	< 0.74	< 0.75	< 0.76
SZ Clusters & CFHTLensing								
Σm_ν [eV]	< 0.36	< 0.27	$0.21^{+013}_{-0.13}$	< 0.32	< 0.30	< 0.31	< 0.28	< 0.31
m_a [eV]	< 1.08	< 1.09	< 0.88	< 0.81	< 0.77	< 1.12	$0.63^{+0.47}_{-0.49}$	$0.58^{+0.50}_{-0.48}$
SZ Clusters								
Σm_ν [eV]	< 0.36	< 0.27	$0.20^{+013}_{-0.14}$	< 0.32	< 0.30	< 0.31	< 0.27	< 0.31
m_a [eV]	< 1.07	< 1.07	< 0.87	< 0.81	< 0.77	< 1.10	$0.62^{+0.46}_{-0.48}$	$0.57^{+0.50}_{-0.47}$

For these datasets there is an evidence at more than 3σ for a neutrino mass of 0.2eV

No evidence for neutrino and axion masses simultaneously!

E. Giusarma, E. Di Valentino, M. Lattanzi, A. Melchiorri and O. Mena, Phys. Rev. D90 (2014), 043507

Axion Cold Dark Matter

For temperatures between the energy scale f_a and the QCD phase transition Λ_{QCD}, the axion is a massless particle, then the axion acquires a mass via instanton effects. The effective potential V for the axion field a(x) is generated through non-pertubative QCD effects, and may be written as

$$V(a) = f_{\rm a}^2 m_{\rm a}^2(T)\left[1 - \cos\left(\frac{a}{f_{\rm a}}\right)\right]$$

Introducing the misalignment angle $\theta = a/f_a$, the field evolves according to the Klein-Gordon equation on a flat Friedmann-Robertson-Walker background:

$$\ddot{\theta} + 3H\dot{\theta} + m_{\rm a}^2(T)\theta = 0$$

with

$$m_{\rm a} \simeq 6.2\,\mu\text{eV}\left(\frac{f_{\rm a}}{10^{12}\,\text{GeV}}\right)^{-1}$$

Axion Cold Dark Matter

The PQ symmetry breaking can occur before or after inflation:

$$f_{\mathrm{a}} < \left(\frac{H_I}{2\pi}\right)$$

- If the PQ symmetry is broken after inflation, there are no axion isocurvature perturbations since there are not axion quantum fluctuations;

- If the PQ symmetry is broken before or during inflation, there will exist, together with the standard adiabatic perturbations generated by the inflaton field, axion isocurvature perturbations, associated to quantum fluctuations in the axion field.

$$f_{\mathrm{a}} > \left(\frac{H_I}{2\pi}\right)$$

Axion Cold Dark Matter

The PQ symmetry breaking can occur before or after inflation:

$$f_a < \left(\frac{H_I}{2\pi}\right)$$

- If the PQ symmetry is broken after inflation, there are no axion isocurvature perturbations since there are not axion quantum fluctuations.

  The total axion cold dark matter density $\Omega_a h^2$ is the sum of two contributions:

- the misalignment mechanism

$$\Omega_{a,\mathrm{mis}} h^2 = \begin{cases} 0.236 \langle \theta_i^2 f(\theta_i) \rangle \left(\frac{f_a}{10^{12}\ \mathrm{GeV}}\right)^{7/6} & f \lesssim \hat{f}_a \\ 0.0051 \langle \theta_i^2 f(\theta_i) \rangle \left(\frac{f_a}{10^{12}\ \mathrm{GeV}}\right)^{3/2} & f \gtrsim \hat{f}_a \end{cases}$$

$$\hat{f}_a = 9.91 \times 10^{16}\ \mathrm{GeV}$$

Axion Cold Dark Matter

The PQ symmetry breaking can occur before or after inflation:

$$f_{\mathrm{a}} < \left(\frac{H_I}{2\pi}\right)$$

- If the PQ symmetry is broken after inflation, there are no axion isocurvature perturbations since there are not axion quantum fluctuations.

  The total axion cold dark matter density $\Omega_a h^2$ is the sum of two contributions:

- the misalignment mechanism

$$\Omega_{\mathrm{a,mis}} h^2 = \begin{cases} 0.236 \boxed{\langle \theta_i^2 f(\theta_i) \rangle} \left(\frac{f_{\mathrm{a}}}{10^{12}\ \mathrm{GeV}} \right)^{7/6} & f \lesssim \hat{f}_a \\ 0.0051 \langle \theta_i^2 f(\theta_i) \rangle \left(\frac{f_{\mathrm{a}}}{10^{12}\ \mathrm{GeV}} \right)^{3/2} & f \gtrsim \hat{f}_a \end{cases}$$

average of all possible initial values of a uniform distribution

$$\boxed{\langle \theta_i^2 f(\theta_i) \rangle} = \frac{1}{2\pi} \int_{-\pi}^{\pi} \theta_i^2 f(\theta_i) d\theta_i = 8.77$$

Axion Cold Dark Matter

The PQ symmetry breaking can occur before or after inflation:

$$f_{\mathrm{a}} < \left(\frac{H_I}{2\pi}\right)$$

- If the PQ symmetry is broken after inflation, there are no axion isocurvature perturbations since there are not axion quantum fluctuations.

  The total axion cold dark matter density $\Omega_a h^2$ is the sum of two contributions:

- the misalignment mechanism

$$\Omega_{\mathrm{a,mis}} h^2 = 2.07 \left(\frac{f_{\mathrm{a}}}{10^{12}\ \mathrm{GeV}}\right)^{7/6}$$

$$\langle \theta_i^2 f(\theta_i) \rangle = \frac{1}{2\pi} \int_{-\pi}^{\pi} \theta_i^2 f(\theta_i) d\theta_i = \boxed{8.77}$$

$$m_{\mathrm{a}}'' = m_{\mathrm{a}} \times \boxed{\left(\frac{\pi^2/3}{8.77}\right)}^{6/7} = m_{\mathrm{a}} \times\ 0.43$$

If anharmonic effects are neglected (i.e. $f(\theta_i)=1$), the factor 8.77 should be replaced by the standard $\pi^2/3$, changing the cold dark matter axion population and consequently the cosmological constraints presented here.

Axion Cold Dark Matter

The PQ symmetry breaking can occur before or after inflation:

$$f_{\rm a} < \left(\frac{H_I}{2\pi}\right)$$

- If the PQ symmetry is broken after inflation, there are no axion isocurvature perturbations since there are not axion quantum fluctuations.

  The total axion cold dark matter density $\Omega_a h^2$ is the sum of two contributions:

- the misalignment mechanism
- and the axionic string decays

$$\Omega_{\rm a} h^2 \quad = \quad 2.07\,(1 \ + \ \alpha_{\rm dec})\left(\frac{f_{\rm a}}{10^{12}\ {\rm GeV}}\right)^{7/6}$$

$$\alpha_{\rm dec} = 0.164$$

where α_{dec} is the ratios between the two contributions.

Axion Cold Dark Matter

The PQ symmetry breaking can occur before or after inflation:

$$f_{\rm a} < \left(\frac{H_I}{2\pi}\right)$$

- If the PQ symmetry is broken after inflation, there are no axion isocurvature perturbations since there are not axion quantum fluctuations.

  The total axion cold dark matter density $\Omega_a h^2$ is the sum of two contributions:

- the misalignment mechanism
- and the axionic string decays

$$\Omega_{\rm a} h^2 \quad = \quad 2.07\,(1 \ + \ \alpha_{\rm dec})\left(\frac{f_{\rm a}}{10^{12}\ \mathrm{GeV}}\right)^{7/6}$$

$$\alpha_{\rm dec} = 0.164$$

$$m_a \longrightarrow m_{\rm a}' = m_{\rm a}\left[\frac{(1+\alpha_{\rm dec})}{(1+0.164)}\right]^{6/7}$$

Axion Cold Dark Matter

If the axion created non-thermally in the early Universe through the misalignment mechanism and the decay of axionic strings, we can constrain the "axion dark matter" scenario in which the PQ symmetry is broken after inflation, using the most precise CMB data available to date.

$$\Omega_{\mathrm{a}} h^2 = 2.41 \left(\frac{f_{\mathrm{a}}}{10^{12}\mathrm{GeV}} \right)^{7/6}$$

We consider the hypothesis that the axion accounts for all the CDM present in the Universe, i.e $\Omega_{CDM} = \Omega_{a,mis}$.

Axion Cold Dark Matter

Planck+WP

Parameter	ADM+r	ADM+r $+N_{\rm eff}$	ADM+r $+\sum m_\nu$	ADM+r $+\sum m_\nu + N_{\rm eff}$	ADM+r $+\, m_s^{\rm eff} + N_{\rm eff}$	ADM+r $+w$	ADM+r $+\, n_t$	ADM+r $+\, dn_s/d\ln k$
$\Omega_{\rm b}h^2$	0.02204 ± 0.00028	0.02261 ± 0.00043	0.02189 ± 0.00033	0.02245 ± 0.00047	0.02246 ± 0.00039	0.02208 ± 0.00028	0.02211 ± 0.00029	0.02229 ± 0.00031
$\Omega_{\rm a}h^2$	0.1194 ± 0.0027	0.1280 ± 0.0054	0.1203 ± 0.0029	0.1277 ± 0.0054	0.1275 ± 0.0055	0.1192 ± 0.0026	0.1206 ± 0.0030	0.1198 ± 0.0027
θ	1.04127 ± 0.00064	1.04053 ± 0.00072	1.04097 ± 0.00070	1.04039 ± 0.00073	1.04040 ± 0.00074	1.04132 ± 0.00063	1.04117 ± 0.00063	1.04133 ± 0.00064
τ	0.089 ± 0.013	0.097 ± 0.015	0.089 ± 0.013	0.096 ± 0.015	0.096 ± 0.014	0.089 ± 0.013	0.089 ± 0.013	0.100 ± 0.016
n_s	0.9614 ± 0.0075	0.991 ± 0.018	0.9576 ± 0.0088	0.985 ± 0.019	0.982 ± 0.018	0.9617 ± 0.0073	0.9615 ± 0.0074	0.9572 ± 0.0080
$log[10^{10}A_s]$	3.086 ± 0.025	3.122 ± 0.033	3.086 ± 0.025	3.119 ± 0.033	3.119 ± 0.032	3.087 ± 0.024	3.149 ± 0.026	3.114 ± 0.031
H_0[km/s/Mpc]	67.4 ± 1.2	73.2 ± 3.5	64.5 ± 3.3	70.4 ± 4.7	70.2 ± 3.4	84 ± 10	67.0 ± 1.2	67.5 ± 1.2
r	< 0.12	< 0.19	< 0.13	< 0.19	< 0.18	< 0.13	< 0.93	< 0.23
$m_{\rm a}(\mu eV)$	$\boxed{81.5 \pm 1.6}$	$\boxed{76.8 \pm 2.8}$	$\boxed{81.0 \pm 1.6}$	$\boxed{77.0 \pm 2.7}$	$\boxed{77.1 \pm 2.9}$	$\boxed{81.6 \pm 1.5}$	$\boxed{80.8 \pm 1.7}$	$\boxed{81.3 \pm 1.6}$
$N_{\rm eff}$	(3.046)	3.79 ± 0.41	(3.046)	3.71 ± 0.41	3.72 ± 0.37	(3.046)	(3.046)	(3.046)
$\sum m_\nu(eV)$	(0.06)	(0.06)	< 0.97	< 0.83	(0.06)	(0.06)	(0.06)	(0.06)
w	(-1)	(-1)	(-1)	(-1)	(-1)	-1.50 ± 0.31	(-1)	(-1)
$m_s^{\rm eff}(eV)$	(0)	(0)	(0)	(0)	< 0.87	$< (0)$	(0)	(0)
n_t	(0)	(0)	(0)	(0)	(0)	(0)	2.19 ± 0.87	(0)
$dn_s/d\ln k$	(0)	(0)	(0)	(0)	(0)	(0)	(0)	-0.022 ± 0.011

Considering also extended scenario we obtain an axion with mass in the range 70-80 μeV.

E. Di Valentino, E. Giusarma, M. Lattanzi, A. Melchiorri, O. Mena, Phys. Rev. D90 (2014), 043534

Axion Cold Dark Matter

We find that, in the minimal ADM scenario, the largest dataset including the precise distance BAO constraints from the BOSS Data Release 11 (DR11), implies

$$m_{\mathrm{a}} = 82.2 \pm 1.1\,\mu\mathrm{eV}$$

$$f_{\mathrm{a}} = (7.54 \pm 0.10) \times 10^{10}\,\mathrm{GeV}$$

- while with an additional number of relativistic degrees of freedom N_{eff}

$$m_{\mathrm{a}} = 76.6 \pm 2.6\,\mu\mathrm{eV}$$

$$f_{\mathrm{a}} = (8.08 \pm 0.27) \times 10^{10}\,\mathrm{GeV}$$

$$N_{\mathrm{eff}} = 3.69 \pm 0.30$$

E. Di Valentino, E. Giusarma, M. Lattanzi, A. Melchiorri, O. Mena, Phys. Rev. D90 (2014), 043534

Axion Cold Dark Matter

- The search for axion dark matter is also the target of laboratory experiments like the Axion Dark Matter eXperiment (ADMX), that uses a tunable microwave cavity positioned in a high magnetic field to detect the conversion of axions into photons. ADMX has been operating in the range 0.3 - 1 GHz, thus being able to exclude DM axions in the mass range between 1.9 and 3.53 μeV.

- To reach the typical masses found in our study, this should be enhanced at a resonant frequency of 20 GHz, if the PQ symmetry is broken after inflation.

- A smaller experiment called ADMX-HF is currently being built, that will allow to probe the 4 - 40 Ghz range, thus being in principle sensitive to axion masses in the 100 μeV range, allowing to directly test the ADM scenario.

Axion Cold Dark Matter

How are the reported results affected by theoretical uncertainties?

We know nothing about the fraction of dark matter provided by misalignment-produced axions. In this case we can note that

$$\Omega_{\rm a,mis} \leq \Omega_{\rm a} \leq \Omega_{\rm dm}$$

from which it follows that the values reported in the tables (divided by a factor $1.164^{6/7}$ to consider only the misaligment contribution to the total) can be considered as lower bounds on the axion mass. In other words, we can put conservative lower limits to the axion mass by requiring only that the density of misalignment-produced axions does not exceed the total dark matter density.

Axion Cold Dark Matter

How are the reported results affected by theoretical uncertainties?

Moreover, the axion abundance depends, among others, on the details of the QCD phase transition through the temperature-dependent axion mass:

$$m_{\rm a}(T) = \begin{cases} C m_{\rm a}(T=0)(\Lambda_{\rm QCD}/T)^4 & T \gtrsim \Lambda_{\rm QCD} \\ m_{\rm a}(T=0) & T \lesssim \Lambda_{\rm QCD} \end{cases}$$

where $C = 0.018$ is a model dependent factor and we have assumed in our analysis $\Lambda_{QCD}=200$ *MeV.* The zero-temperature mass $m_a(T = 0)$ is related to the PQ scale from the previous:

$$m_{\rm a} \simeq 6.2\,\mu{\rm eV}\left(\frac{f_{\rm a}}{10^{12}\,{\rm GeV}}\right)^{-1}$$

Axion Cold Dark Matter

How are the reported results affected by theoretical uncertainties?

We have run additional chains substituting the relationships that assumes Λ_{QCD}=200 *MeV*

$$\Omega_{\mathrm{a,mis}} h^2 = 2.07 \left(\frac{f_{\mathrm{a}}}{10^{12}\ \mathrm{GeV}} \right)^{7/6}$$

with the relation derived by Bae, Huh & Kim considering three different values for Λ_{QCD}, namely Λ_{QCD}=320, 380, 440 *MeV.*

$\Lambda_{\mathrm{QCD}}\ [MeV]$	$m_a\ [\mu eV]$
200	81.5 ± 1.6
320	75.6 ± 1.4
380	69.0 ± 1.3
440	63.7 ± 1.2

Neutrino isocurvature

The present data are consistent with an adiabatic and gaussian universe, but the sensitivity is such that we cannot exclude the presence of non-adiabatic primordial isocurvature perturbation modes.

In the curvaton model, while the exponential expansion is driven by the inflaton field, the primordial fluctuations are generated by a different field called "curvaton".

After the inflaton decay, the isocurvature perturbation produced initially by the curvaton is converted in an adiabatic component. Some residual isocurvature perturbation is therefore expected in the cosmological fluids (cold dark matter, baryons and neutrinos).

In case of a non-vanishing neutrino chemical potential, neutrino isocurvature density perturbations (NID) are expected, that could bias the value of N_{eff}.

Neutrino isocurvature

Probing neutrino isocurvature density perturbation in the curvaton scenario is complementary to constrain the lepton number in the neutrino sector.

Actually NID perturbations necessarily implies a non zero lepton asymmetry for the neutrino $n_L \equiv n_\nu - n_{\bar{\nu}}$

unless there is an exact cancellation of the asymmetries in the three flavours.

In fact the relativistic neutrinos will follow an equilibrium distribution function as

$$f_i(E) = \left[\exp(E/T_\nu \mp \xi_i)\right]^{-1}$$

where the minus (plus) sign is for neutrinos (antineutrinos).

$$\xi_i = \mu_i/T_\nu$$

Chemical potential

Neutrino isocurvature

The energy density $\rho_i \equiv \rho_{\nu_i} + \rho_{\bar{\nu}_i}$

will be:

$$\rho_i = \frac{7\pi^2}{120} A_i T_\nu^4 = \frac{7}{8} A_i \left(\frac{T_\nu}{T_\gamma}\right)^4 \rho_\gamma$$

where

$$A_i \equiv \left[1 + \frac{30}{7}\left(\frac{\xi_i}{\pi}\right)^2 + \frac{15}{7}\left(\frac{\xi_i}{\pi}\right)^4\right]$$

Neutrino isocurvature

The energy density $\rho_i \equiv \rho_{\nu_i} + \rho_{\bar{\nu}_i}$

will be: $\rho_i = \frac{7\pi^2}{120} A_i T_\nu^4 = \boxed{\frac{7}{8} A_i \left(\frac{T_\nu}{T_\gamma}\right)^4 \rho_\gamma}$

$$\rho_r = (1 + \boxed{N_{eff} \frac{7}{8}\left(\frac{4}{11}\right)^{4/3})\rho_\gamma}$$

$$\boxed{N_{eff} = \Sigma_i A_i + 0.046}$$

Neutrino isocurvature

The gauge invariant variable ζ_i describes the curvature perturbation on slices of uniform total density for each of the i-th energy component:

$$\zeta_i = -\psi - H\frac{\delta\rho_i}{\dot{\rho}_i}$$

For an adiabatic mode we have $\zeta_i = \zeta$ for all components.

For the isocurvature fluctuation S_i is given by the relative entropy fluctuation with respect to photons:

$$\boxed{\mathcal{S}_i \equiv 3(\zeta_i - \zeta_\gamma)}$$

$$\Rightarrow \quad \boxed{\mathcal{S}_\nu = 3(\zeta_\nu - \zeta_\gamma) \simeq \frac{\sum_i \delta N_{\rm eff}^{(i)}}{4N_{\rm eff}}}$$

Neutrino isocurvature

In CMB studies the “non-adiabaticity" of perturbations is expressed, as the following ratio:

$$\boxed{\frac{\alpha^{NID}(k_0)}{1-\alpha^{NID}(k_0)} \equiv \frac{P_{\mathcal{S}}(k_0)}{P_{\zeta}(k_0)}}$$

where $P_S(k_0)$ is the power spectrum of isocurvature perturbations to the curvature perturbation spectrum $P_\zeta(k_0)$, and, in our analysis, k_0=0.05 Mpc is the fixed pivot wave number at which they are evaluated.

Another necessary parameter to consider is the cross-correlation coefficient between the adiabatic and isocurvature modes, defined as:

$$\boxed{\beta = \frac{P_{\zeta\mathcal{S}}(k_0)}{\sqrt{P_{\mathcal{S}}(k_0)P_{\zeta}(k_0)}}}$$

where $P_{\zeta S}(k_0)$ is the cross-correlation power spectrum. With this convention, the adiabatic and isocurvature perturbations are totally anti-correlated taking β=-1 and totally correlated taking β=1 in the curvaton scenario.

Neutrino isocurvature

Since we will consider only totally correlated or anti-correlated spectra, in order to simplify the notation, we will vary only one parameter α^{NID} that is ever defined positive, and we replace β=1 with the sign(α^{NID}):

$$C_\ell = (1-\alpha^{NID})C_\ell^{ad} + \alpha^{NID} C_\ell^{nid} + \\ + 2 sign(\alpha^{NID})\sqrt{\alpha^{NID}(1-\alpha^{NID})C_\ell^{corr}}$$

NID amplitude

$\boxed{\alpha^{NID}}$

> 0 totally correlated

< 0 totally anticorrelated

Neutrino isocurvature

Parameter	Planck+WP	Planck+WP+HST
$\Omega_b h^2$	0.02215 ± 0.00050	0.02260 ± 0.00033
$\Omega_c h^2$	0.1222 ± 0.0068	0.1273 ± 0.0056
θ	1.0405 ± 0.0010	1.0408 ± 0.0011
τ	0.094 ± 0.015	0.099 ± 0.015
n_s	0.966 ± 0.021	0.987 ± 0.012
$log[10^{10} A_s]$	3.115 ± 0.035	3.122 ± 0.037
H_0[km/s/Mpc]	68.7 ± 3.9	72.5 ± 2.2
$N_{\rm eff}$	3.26 ± 0.48	3.70 ± 0.30
α^{NID}	-0.0031 ± 0.0053	0.0002 ± 0.0031

The Planck+WP data does not show any indication for NID or for a larger value for $N_{\rm eff}$.

We have a cosmological degeneracy: models with smaller values for $N_{\rm eff}$ are more consistent with the CMB observations when NID is totally anticorrelated.

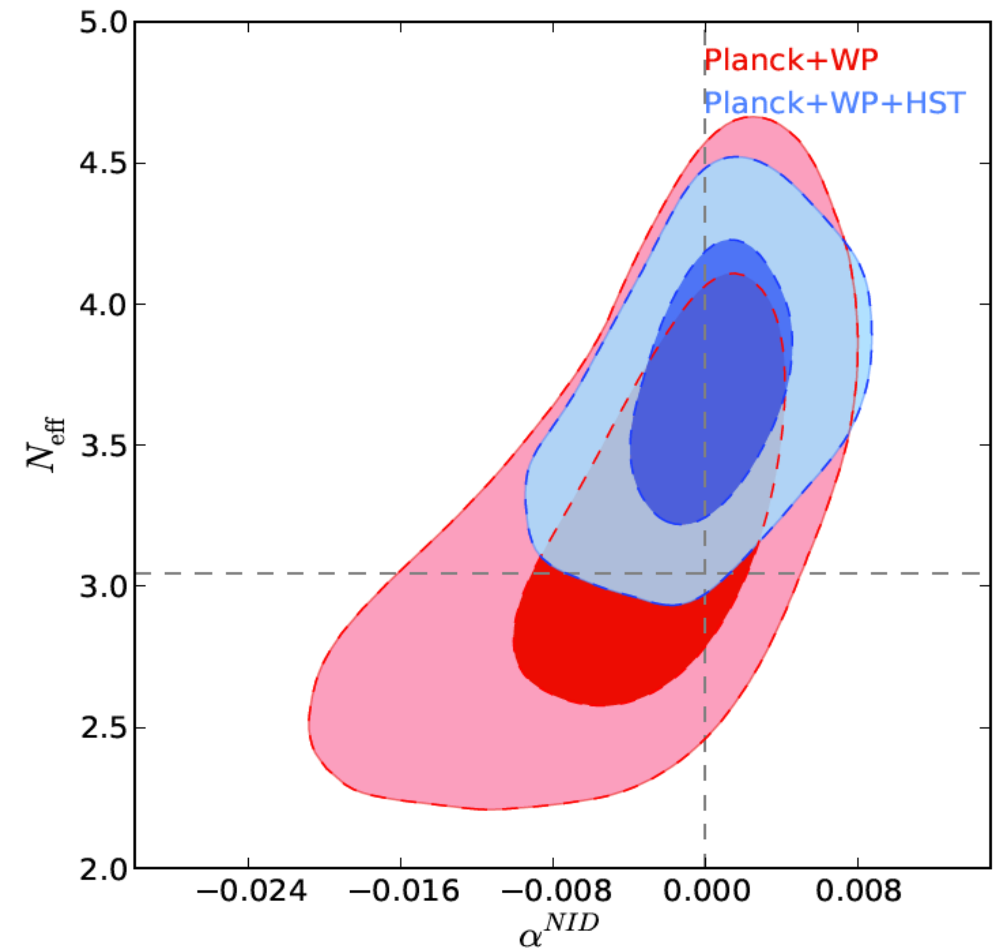

FIG. 1. 68% and 95% c.l. likelihood contours for Planck+WP and Planck+WP+HST in the N_{eff} vs. α^{NID} plane. Note the small correlation between the two parameters.

Neutrino isocurvature

Parameter	Planck+WP	Planck+WP+HST
$\Omega_b h^2$	0.02215 ± 0.00050	0.02260 ± 0.00033
$\Omega_c h^2$	0.1222 ± 0.0068	0.1273 ± 0.0056
θ	1.0405 ± 0.0010	1.0408 ± 0.0011
τ	0.094 ± 0.015	0.099 ± 0.015
n_s	0.966 ± 0.021	0.987 ± 0.012
$log[10^{10} A_s]$	3.115 ± 0.035	3.122 ± 0.037
H_0[km/s/Mpc]	68.7 ± 3.9	72.5 ± 2.2
$N_{\rm eff}$	3.26 ± 0.48	$\boxed{3.70 \pm 0.30}$
α^{NID}	-0.0031 ± 0.0053	$\boxed{0.0002 \pm 0.0031}$

Including HST reduces the error bars on the NID component while providing an indication for a non-standard value for $N_{\rm eff}$ at more than two standard deviations.

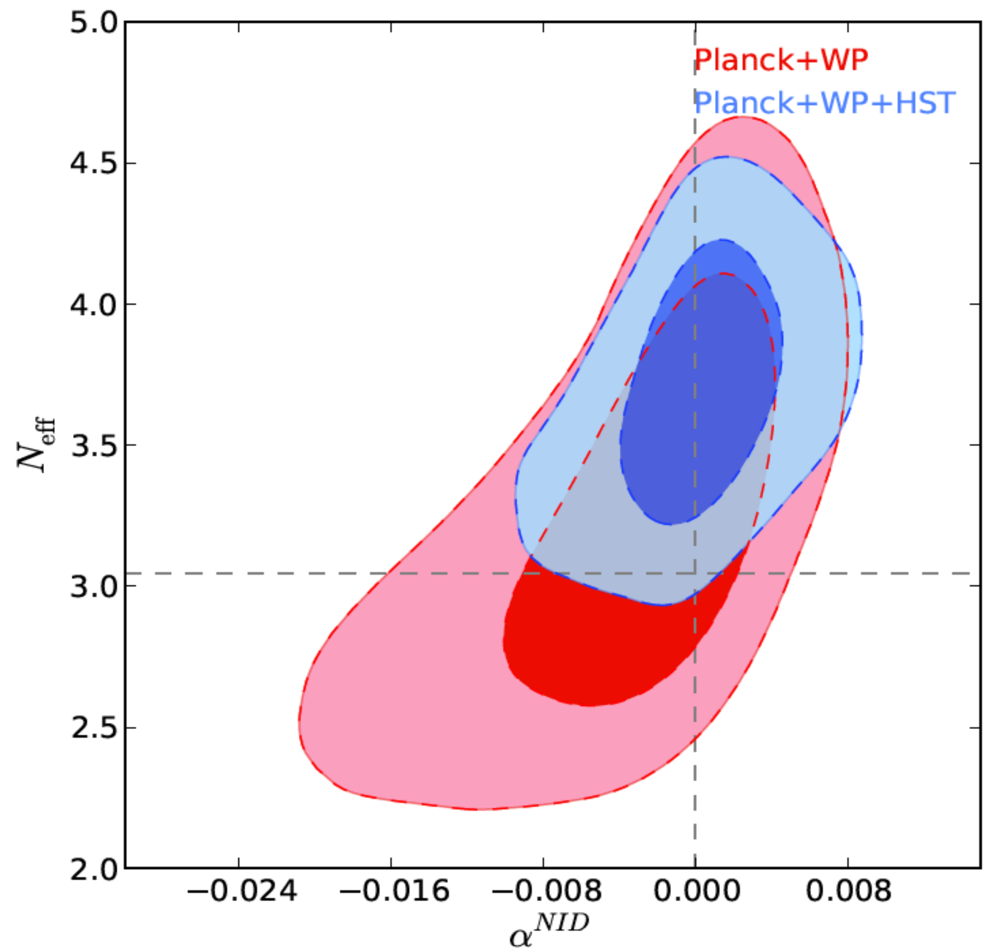

FIG. 1. 68% and 95% c.l. likelihood contours for Planck+WP and Planck+WP+HST in the N_{eff} vs. α^{NID} plane. Note the small correlation between the two parameters.

BBN

Big Bang Nucleosynthesis (BBN) offers one of the most powerful methods to test the validity of the cosmological model around the MeV energy scale. We can derive:

$$N_{\rm eff} = \begin{cases} 3.41 \pm 0.30, & Y_{\rm P} \text{ (Aver et al.)}, \\ 3.43 \pm 0.34, & y_{\rm DP} \text{ (Iocco et al.)}, \\ 3.02 \pm 0.27, & y_{\rm DP} \text{ (Pettini and Cooke)}. \end{cases}$$

([Planck Collaboration], arXiv:1303.5076)

using the primordial abundance of light elements.

BBN

Big Bang Nucleosynthesis (BBN) offers one of the most powerful methods to test the validity of the cosmological model around the MeV energy scale.

BBN relates key cosmological parameters:

- the energy density in baryons, $\Omega_b h^2$
- the effective neutrino number, N_{eff}

⇨ to the primordial abundance of light elements.

BBN

Big Bang Nucleosynthesis (BBN) offers one of the most powerful methods to test the validity of the cosmological model around the MeV energy scale.

The deuterium primordial abundance $^2H/H$ is:

- a rapidly decreasing function of $\Omega_b h^2$
- a growing function of N_{eff}

Deuterium abundance

Assuming the standard cosmological model, we show in E. Di Valentino et al., Phys. Rev. D90 (2014), 023543, that combining

- the Planck data
- the recent deuterium abundance measurements in metal-poor damped Lyman-alpha systems

we have independent information on the cross section of the radiative capture reaction $d(p;\gamma)^3He$ converting deuterium into helium.

Deuterium abundance

Assuming a given cosmological scenario and standard BBN dynamics, it's possible to infer indirectly from Planck data the abundance of primordial nuclides with exquisite precision.

From the Planck constraint on the baryon density:

$$\Omega_b h^2 = 0.02207 \pm 0.00027$$

using the public BBN code PArthENoPE we have:

$$^2\mathrm{H/H} = (2.65 \pm 0.07) \cdot 10^{-5} \quad (68\% \text{ C.L.})$$

Cosmological determination

Deuterium abundance

A new analysis of all known deuterium absorption-line systems, including some new data from very metal-poor Lyman-alpha systems at redshift z = 3.06726 (visible in the spectrum of the quasar QSO SDSS J1358+6522) and at redshift z = 3.04984 (seen in QSO SDSS J1419+0829), gives:

$$^{2}\mathrm{H}/\ \mathrm{H} = (2.53 \pm 0.04) \cdot 10^{-5} \quad (68\%\ \mathrm{C.L.})$$

Astrophysical determination

Deuterium abundance

Planck → $^{2}\mathrm{H}/\mathrm{H} = (2.65 \pm 0.07) \cdot 10^{-5} \quad (68\%\ \mathrm{C.L.})$

Lyman-alpha → $^{2}\mathrm{H}/\ \mathrm{H} = (2.53 \pm 0.04) \cdot 10^{-5} \quad (68\%\ \mathrm{C.L.})$

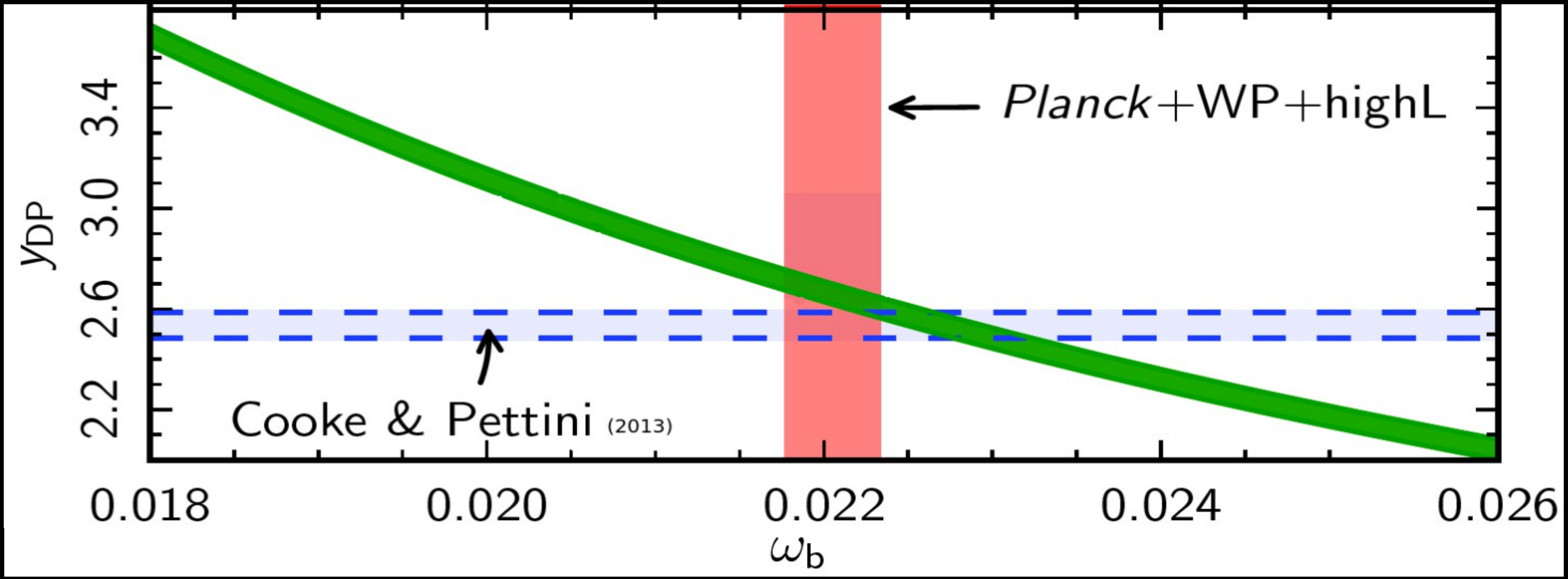

Deuterium abundance

Planck → $^{2}\mathrm{H}/\mathrm{H} = (2.65 \pm 0.07) \cdot 10^{-5} \quad (68\%\ \mathrm{C.L.})$

Lyman-alpha → $^{2}\mathrm{H}/\ \mathrm{H} = (2.53 \pm 0.04) \cdot 10^{-5} \quad (68\%\ \mathrm{C.L.})$

These two deuterium abundance determinations, while broadly consistent, are off by about two standard deviations.

This small tension might well be the result of small experimental systematics in these measurements....

...or the current BBN calculations could also be plagued by systematics in the experimental determination of nuclear rates.

d(p;γ)^{3}He

The main uncertainty for standard BBN calculations of ^{2}H comes from the rate R2 of the radiative capture reaction *d(p;γ)^{3}He*, measured from nuclear experimental data.

A reliable *ab initio* nuclear theory calculation of this cross section is systematically larger than the best-fit value derived from the experimental data in the BBN energy range *[30-300 keV]*. Further data on R2 in the relevant energy range might be expected from experiments such as LUNA.

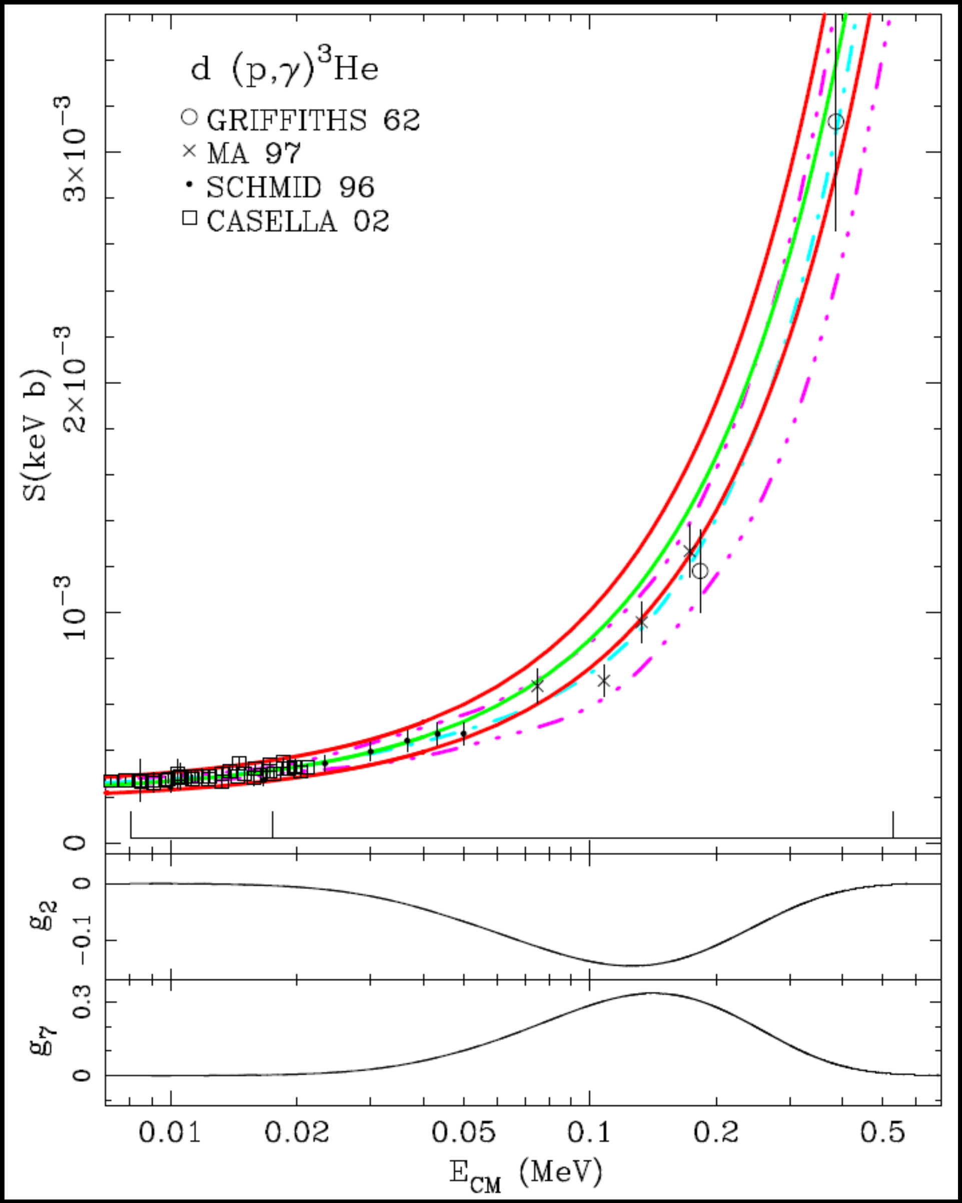

$d(p;\gamma)^3He$

Could be this the way to reconcile the different values of $^2H/H$ measured in astrophysical and cosmological data?

If we put the theoretical estimate of R_2 in a BBN code, we find that more deuterium is destroyed for the same value of the cosmological baryon density. In this way, the predicted primordial ^2H abundance by Planck results to be smaller, i.e. more in agreement with the astrophysical estimate.

Planck new

$$^2\mathrm{H}/\mathrm{H} = (2.58 \pm 0.07) \cdot 10^{-5} \quad (68\%\ \mathrm{C.L.})$$

Lyman-alpha

$$^2\mathrm{H}/\ \mathrm{H} = (2.53 \pm 0.04) \cdot 10^{-5} \quad (68\%\ \mathrm{C.L.})$$

$d(p;\gamma)^3He$

We analyzed the Planck data considering the rate of the radiative capture reaction $d(p;\gamma)^3He$ as a free input parameter.

Actually the present CMB data are powerful enough to provide information on nuclear rates.

Our aim is to find which value of this cross section, brings the Planck predictions in better agreement with the deuterium measurements.

We find that our results give independent support to the theoretical calculation: the rate of the radiative capture reaction $d(p;\gamma)^3He$ is larger than measured from the nuclear experiments.

We parametrize the generic $R_2(T)$ in terms of an overall rescaling factor A_2

$$R_2(T) = A_2\, R_2^{ex}(T)$$

A_2

Parameter	Planck+WP +BBN	Planck+WP +BBN+BAO
$\Omega_b h^2$	0.02202 ± 0.00028	0.02209 ± 0.00025
$\Omega_c h^2$	0.1200 ± 0.0026	0.1188 ± 0.0017
θ	1.04129 ± 0.00063	1.04144 ± 0.00058
τ	0.089 ± 0.013	0.091 ± 0.013
n_s	0.9599 ± 0.0073	0.9625 ± 0.0058
$\log[10^{10} A_s]$	3.089 ± 0.025	3.089 ± 0.025
H_0[km/s/Mpc]	67.2 ± 1.2	67.74 ± 0.78
A_2	1.155 ± 0.082	1.138 ± 0.076

We find that data provide an indication for A_2 being greater than one, at about 2σ, even when adding the BAO dataset.

E. Di Valentino et al., Phys. Rev. D90 (2014), 023543

A_2-N_{eff}

Parameter	Planck+WP +BBN	Planck+WP +BBN+HST	Planck+WP +BBN+BAO
$\Omega_b h^2$	0.02241 ± 0.00042	0.02261 ± 0.00031	0.02233 ± 0.00029
$\Omega_c h^2$	0.1263 ± 0.0055	0.1281 ± 0.0049	0.1251 ± 0.0051
τ	0.096 ± 0.015	0.099 ± 0.014	0.094 ± 0.013
n_s	0.979 ± 0.017	0.988 ± 0.011	0.974 ± 0.010
$\log[10^{10} A_s]$	3.117 ± 0.034	3.128 ± 0.030	3.109 ± 0.029
H_0[km/s/Mpc]	71.0 ± 3.2	72.8 ± 2.0	70.1 ± 1.9
$N_{\rm eff}$	3.56 ± 0.40	3.76 ± 0.27	3.43 ± 0.30
A_2	1.29 ± 0.15	1.33 ± 0.14	1.26 ± 0.14

The preference for A_2>1 is robust against the extension. When HST is included the indication is at about 2.5σ.

E. Di Valentino et al. arXiv:1404.7848

A_2-N_{eff}

Parameter	Planck+WP +BBN	Planck+WP +BBN+HST	Planck+WP +BBN+BAO
$\Omega_b h^2$	0.02241 ± 0.00042	0.02261 ± 0.00031	0.02233 ± 0.00029
$\Omega_c h^2$	0.1263 ± 0.0055	0.1281 ± 0.0049	0.1251 ± 0.0051
τ	0.096 ± 0.015	0.099 ± 0.014	0.094 ± 0.013
n_s	0.979 ± 0.017	0.988 ± 0.011	0.974 ± 0.010
$\log[10^{10} A_s]$	3.117 ± 0.034	3.128 ± 0.030	3.109 ± 0.029
H_0[km/s/Mpc]	71.0 ± 3.2	72.8 ± 2.0	70.1 ± 1.9
$N_{\rm eff}$	3.56 ± 0.40	3.76 ± 0.27	3.43 ± 0.30
A_2	1.29 ± 0.15	1.33 ± 0.14	1.26 ± 0.14

From this analysis is clear that the $N_{eff} = 3.02 \pm 0.27$ provided by the Planck collaboration, when the deuterium abundance measurements are included, is mostly driven by A_2=1. When A_2 is let free, we have a preference for $N_{eff} > 3.046$.

E. Di Valentino et al. arXiv:1404.7848

A_2-N_{eff}

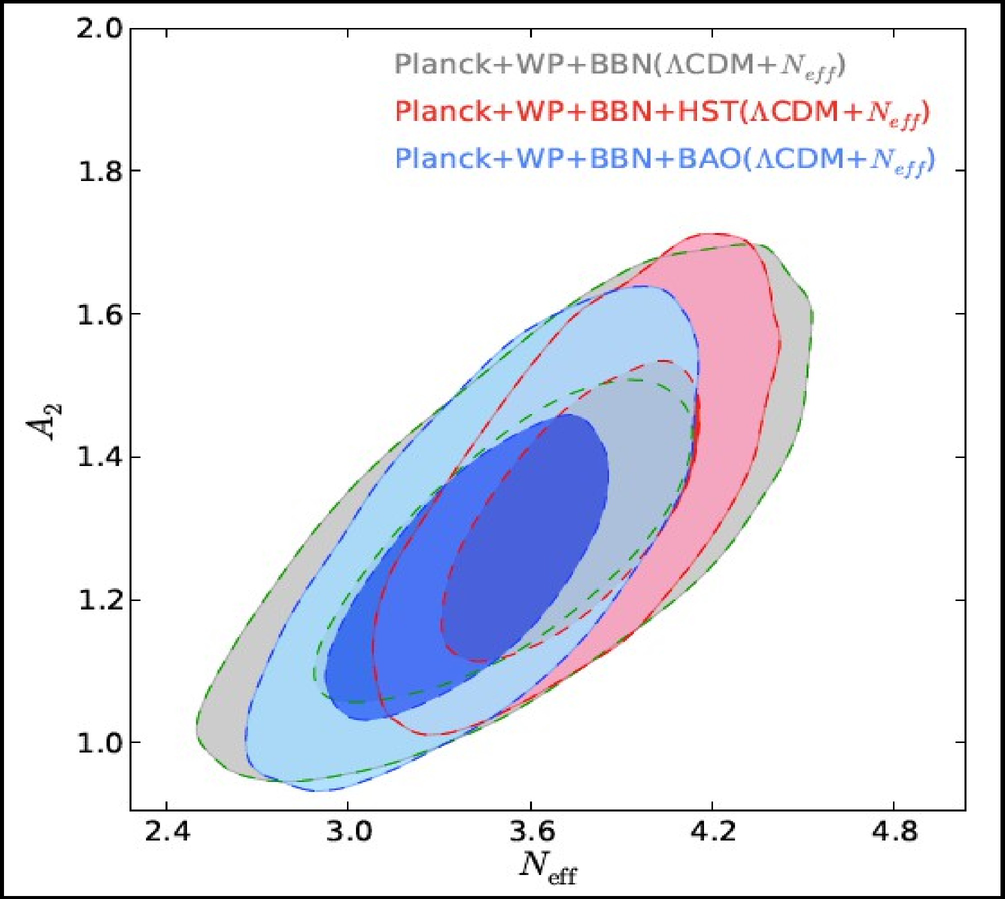

From this analysis is clear that the N_{eff} = 3.02 ± 0.27 provided by the Planck collaboration, when the deuterium abundance measurements are included, is mostly driven by A_2=1. When A_2 is let free, we have a preference for N_{eff} > 3.046.

E. Di Valentino et al. arXiv:1404.7848

A_2-A_L

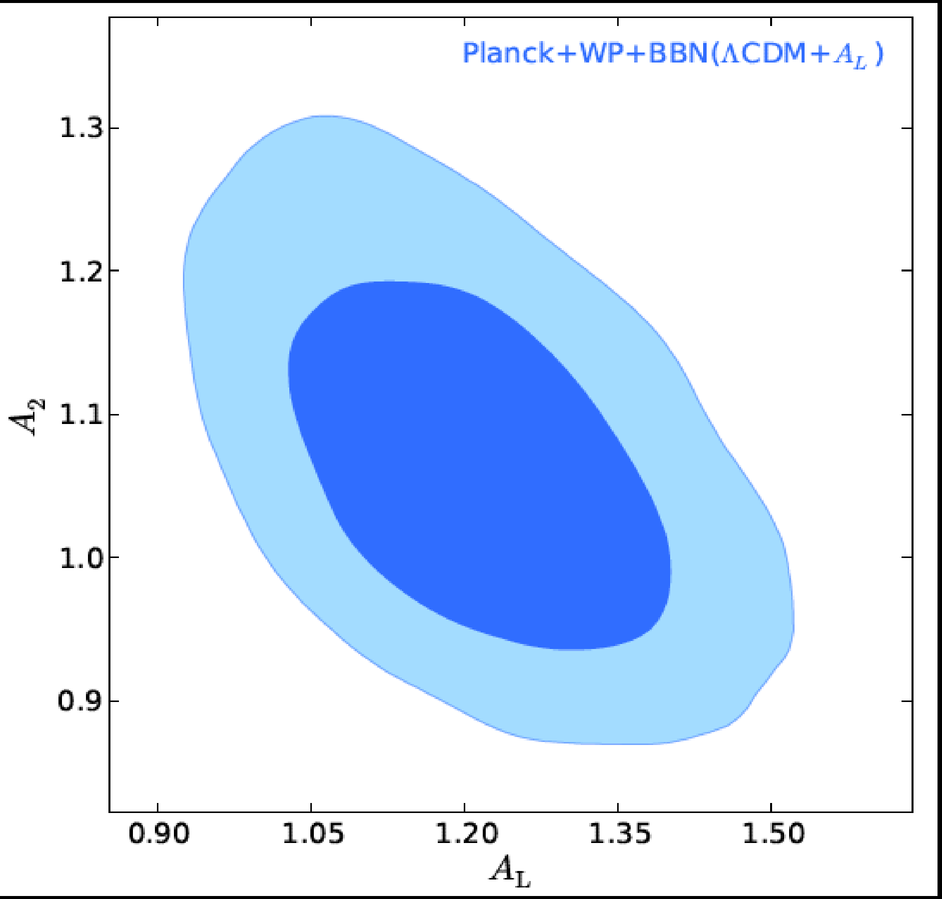

The Planck data prefers $A_L > 1$, but as such, this result has no physical interpretation. When A_L is left free, the A_2 parameter is well compatible with one.

E. Di Valentino et al. arXiv:1404.7848

Conclusions:

- I analyzed the values of N_{eff} arising from the two ground based experiments ACT and SPT combined with WMAP9, and I compared these results with the Planck satellite bounds. Current cosmological data are suggesting both the parameters greater than the standard value, $N_{eff}>3.046$ and $A_L>1$.
- I investigated the constraints on the possible candidates for this dark radiation component $\Delta N_{eff} \equiv N_{eff} - 3.046$, since an excess of dark radiation could be due to the presence of relic relativistic particles beyond the standard model of particle physics (as thermal axions or sterile neutrinos) at recombination epoch. I presented constraints on their masses: $m_a<0.79$eV at 95% c.l. and $m_{eff}<0.29$eV at 95% c.l. for CMB+DR11.
- I considered that this excess could be also due to a non-vanishing neutrino chemical potential, and I explored this possibility in the Curvaton scenario, finding parameters consistent with their standard value $N_{eff}=3.046$ and $\alpha^{NID}=0$.
- I presented the current bounds we found on the total neutrino masses, considering BAO mesurements given by BOSS DR11 combined with other datasets, in several extended cosmological scenarios. We found $\Sigma m_\nu<0.25$eV at 95% c.l. for CMB+DR11.
- I considered also the possibility that non-thermal axions account for all the cold dark matter present in the Universe and I presented the constraints on their masses, finding a mass in the range 70-80 μeV.
- I showed how the accuracy reached by current cosmological data allow us to give independent information on nuclear rates, as the radiative capture reaction $d(p,y)^3He$. We found that a higher rate is favoured from the Planck data, preferring theoretical calculations, that predict this rate about 5-10% higher than what has been measured by laboratory experiments.

Thank you!

eleonora.divalentino@gmail.com

References

- Hinshaw et al., arXiv: 1212.5226
- Sievers et al., arXiv: 1301.0824
- Story et al., arXiv: 1210.7231
- P. A. R. Ade et al. [Planck Collaboration], arXiv: 1303.5076 [astro-ph.CO].
- G. Mangano et al., Nucl. Phys. B 729, 221 (2005) [hep-ph/0506164].
- Hou et al., arXiv:1104.2333v2
- Hou et al., arXiv:1212.6267v1
- Calabrese et al., Phys. Rev. D, 77, 123531
- E. Di Valentino et al., Phys. Rev. D88 (2013) 2, 023501 (2013);
- N. Said et al., Phys. Rev. D88 (2013) 2, 023513;
- J. Lesgourgues and S. Pastor, arXiv:1212.6154 [hep-ph].
- R. D. Peccei and H. R. Quinn, Phys. Rev. Lett. 38, 1440 (1977);
- E. Giusarma et al., Phys. Rev. D90 (2014), 043507;
- L. Visinelli and P. Gondolo, arXiv:1403.4594 [hep-ph];
- D.J. Gross, R.D. Pisarski, and L.G. Yaffe, Rev. Mod. Phys. 53, 43 (1981);
- L. Visinelli and P. Gondolo, Phys. Rev. D 80, 035024 (2009);
- W. J. Percival et al. [SDSS Collaboration] arXiv:0907.1660 [astro-ph.CO]
- N. Padmanabhan et al., arXiv:1202.0090 [astro-ph.CO].
- C. Blake, et al. ArXiv:1108.2635 [astro-ph.CO]
- *F. Beutler, et al. arXiv:1106.3366 [astro-ph.CO]*
- *Aubourg et al., arXiv:1411.1074v1*
- *Dvorkin et al., arXiv:1403.8049*
- L. Anderson, et al. , arXiv:1312.4877 [astro-ph.CO].
- D. Parkinson, et al. ArXiv:1210.2130 [astro-ph.CO]
- A. Conley, et al. arXiv:1104.1443 [astro-ph.CO]
- *A. G. Riess, et al. arXiv:1103.2976 [astro-ph.CO]*
- *P. A. R. Ade et al. [Planck Collaboration], arXiv:1303.5080 [astro-ph.CO].*
- *D. H. Lyth, D. Wands, Phys. Lett. B524, 5-14 (2002)*
- *D. H. Lyth et al., Phys. Rev. D67, 023503 (2003)*
- *E. Di Valentino et al., [arXiv:1111.3810 [astro-ph.CO]*
- *C. Heymans, et al., arXiv:1303.1808 [astro-ph.CO].*
- *R. Cooke, M. Pettini, R. A. Jorgenson, M. T. Murphy and C. C. Steidel, arXiv:1308.3240 [astro-ph.CO].*
- *E. Di Valentino et al., arXiv:1405.1860 [astro-ph.CO]*
- *E. Di Valentino et al., arXiv:1405.5418 [astro-ph.CO]*
- *E. Di Valentino et al., arXiv:1404.7848 [astro-ph.CO]*
- *R. Cooke et al., arXiv:1308.3240 [astro-ph.CO];*
- *L. E. Marcucci et al., Phys. Rev. C 72, 014001 (2005);*
- *K. M. Nollett and G. P. Holder, arXiv:1112.2683 [astro-ph.CO];*
- *O. Pisanti et al., arXiv:0705.0290 [astro-ph]], URL http://parthenope.na.infn.it/;*